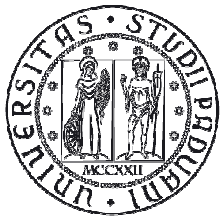

UNIVERSITÀ
DEGLI STUDI
DI PADOVA

Università degli Studi di Padova
Dipartimento di Farmacologia ed Anestesiologia

Scuola di Dottorato di Ricerca in Scienze Farmacologiche
Indirizzo Farmacologia Molecolare e Cellulare
XXII Ciclo

Homotypic fusion of ER membranes requires the dynamin-like GTPase Atlastin

Direttore della Scuola: Prof. Rosa Maria Gaion
Coordinatore d'indirizzo: Prof. Pietro Giusti
Supervisore: Prof. Sergio Bova
Supervisore esterno: Dott. Andrea Daga

Dottorando: Diana Pendin

ABSTRACT

The endoplasmic reticulum (ER) is a subcellular organelle comprised of interconnecting membrane networks. Formation and maintenance of the intricate ER architecture is essential for implementation of the multiple functions served by this organelle. Homotypic membrane fusion underlies both the biogenesis and maintenance of the ER and depends categorically on GTP hydrolysis but does not require cytosolic components, suggesting that a membrane bound GTPase may be responsible for this activity.

Using *in vivo* analysis in *Drosophila* we demonstrate that the GTPase Datlastin, the fly homologue of the dynamin superfamily member atlastin-1 whose mutation causes Hereditary Spastic Paraplegia, is specifically localized on ER membranes. Furthermore, loss of Datlastin causes fragmentation of the ER but does not impair secretory pathway traffic. Datlastin embedded in distinct membranes has the ability to form trans-oligomeric complexes and its overexpression induces enlargement of ER profiles, consistent with excessive fusion of ER membranes. *In vitro* experiments confirm that Datlastin autonomously drives membrane fusion in a GTP dependent fashion. In contrast, GTPase-deficient Datlastin is inactive, unable to form trans-oligomeric complexes due to failure to self-associate, and incapable of promoting fusion *in vitro*. These results demonstrate that Datlastin mediates membrane tethering and fusion and strongly suggest that it is the GTPase activity required for ER homotypic fusion.

ABSTRACT

Il reticolo endoplasmatico (RE) è un organello formato da un complesso network di membrane. La formazione e il mantenimento dell'elaborata architettura del RE è essenziale per lo svolgimento delle numerose funzioni di questo organello. La biogenesi e il mantenimento del RE dipendono dalla capacità delle membrane del RE di fondersi in maniera omotipica. La dipendenza di questo processo dall'idrolisi del GTP, ma non da fattori citosolici, suggerisce che la fusione omotipica sia mediata da una GTPasi di membrana.

Datlastina è l'omologo in *Drosophila* di atlastina-1, GTPasi membro della superfamiglia delle dinamine le cui mutazioni causano l'insorgenza di Paraplegia Spastica Ereditaria nell'uomo. Analisi *in vivo* in *Drosophila* hanno mostrato che Datlastina è localizzata sulla membrana del reticolo endoplasmatico. L'assenza di Datlastina causa frammentazione del RE, ma non blocca il traffico secretorio. Molecole di Datlastina inserite in membrane distinte sono in grado di associarsi in trans e la sovraespressione della proteina *in vivo* induce la formazione di profili di RE allargati, compatibili con una eccessiva fusione delle membrane del RE. Esperimenti *in vitro* hanno confermato che Datlastina è in grado di promuovere autonomamente la fusione di membrane in modo GTP dipendente. Al contrario, Datlastina priva di attività GTPasica è inattiva, incapace di associarsi in trans e di promuovere la fusione delle membrane *in vitro*. Questi risultati dimostrano che Datlastina è in grado di mediare l'avvicinamento e la fusione delle membrane e suggeriscono che costituisca l'attività GTPasica necessaria per la fusione omotipica delle membrane del RE.

1. INTRODUCTION

1.1 MEMBRANE FUSION

1.1.1 General features of membrane fusion

Life in eukaryotes depends on the dynamics of membranous organelles. Every vital process relies on the orderly execution of membrane fusion and fission, from the exquisite compartmental organization of all cells to the precise timing of synaptic transmission in the brain. Membrane fission and fusion processes recur at numerous transport steps to move cargo between intracellular organelles, to transmit information between cells and organs, and to respond to external stimuli. Membrane fission within a single membrane produces transport vesicles or viruses, whose properties usually differ from the compartment of origin. In this process, coat-like structures shape the membrane into symmetric vesicular or tubular structures, sort cargo, and finally physically push the membrane together, to create two separate compartments.

In contrast to membrane fission, fusion merges two compartments, a process that requires specific compartment recognition and a machinery that pulls the membranes together. Numerous membrane-fusion processes have been extensively studied and many molecules involved in fusion have been identified. From these studies it is clear that there are distinct and structurally unrelated membrane-fusion molecules. Despite this, there are general principles that operate in all fusion events.

It is now believed that most, if not all, biological membrane fusion proceeds through a hemifusion intermediate. According to this mechanism, an intermediate stage of membrane fusion is the merger of only the outer monolayers, with full fusion resulting in complete bilayer merging. Membrane-fusion intermediates are regulated by cellular proteins that manifest their activity through the promotion of membrane–membrane proximity, by bending and remodelling membranes, or by acting upstream to regulate the lipid or protein composition of the respective lipid bilayers (Xu *et al.*, 2005).

Several energy barriers have to be overcome for fusion to occur. One energetically demanding process is to bring about the close apposition of two membranes, which requires protein clearance and the bringing together of repulsive membrane charges. The energy barriers related to curvature deformations during hemifusion-stalk and fusion-pore formation and expansion must also be overcome. The role of fusion proteins is to lower these barriers at the appropriate time and place to allow the regulation of the fusion process. Membrane-fusion events generally require also molecules that locally disturb the lipid bilayers (for example, by the induction of extreme membrane curvature) in order to reduce the energy barriers for fusion, and molecules that give directionality to the process. The driving force for membrane fusion can come from many sources, for example from the energy that is derived from protein–lipid interactions or from protein–protein interactions, and ultimately these reactions will have been primed by ATP. Directionality might be achieved by fusion protein folding. In addition, curvature stress that promotes fusion-stalk formation will be relieved during fusion-pore opening and expansion, again giving directionality to the process from the beginning (Chernomordik and Kozlov, 2008; Martens and McMahon, 2008).

Membrane fusion between cells, viruses and cells, or transport vesicles and intracellular organelles employs distinct molecular machines.

1.1.2 Viral membrane fusion

Infection by viruses having lipid-bilayer envelopes proceeds through fusion of the viral membrane with the membrane of the target cell. One or more viral ‘fusion proteins’ facilitate this process. They vary greatly in structure, but all seem to have a common mechanism of action. All viral fusion proteins studied so far have two membrane-interacting elements: a C-terminal transmembrane anchor that holds the protein in the viral membrane and a distinct hydrophobic patch (‘fusion peptide’ or ‘fusion loop(s)’) that ultimately interacts with the target membrane.

In the initial step in the fusion reaction, the fusion protein, responding to binding of a ligand, undergoes a conformational change that extends each subunit toward the target membrane and yields a contact between that membrane and the fusion peptide or loop(s). Then the bridge collapses so that the two membrane-inserted elements (the fusion peptide or loop in the target membrane and the C-terminal transmembrane anchor in the viral membrane) come together. This collapse distorts the two bilayers with a relatively restricted area of close approach. The distortion of the individual membranes lowers the energy barrier between separated and hemifused bilayers so that a hemifusion stalk forms. Then the hemifusion stalk opens to form a transient fusion pore. A final conformational step in the protein refolding renders the open state irreversible, and the pore expands (Harrison, 2008).

1.1.3 Intracellular membrane fusion

Intracellular membrane fusion can either be heterotypic (when a membrane fuses with a dissimilar type of compartment; for example, synaptic vesicle exocytosis) or homotypic (when the same compartment fuses with itself; for example, mitochondrion-mitochondrion fusion).

Much of what is known about intracellular membrane fusion has come from three major approaches: genetic studies in budding yeast, the study of the tightly regulated synaptic fusion machinery and identification of its core components, and lipid-mixing assays aimed at recapitulating the fusion reaction *in vitro*. These studies have led to the conclusion that most intracellular membrane fusion events are carried out by a largely conserved mechanism performed by the SNARE proteins and associated regulatory factors and effector proteins.

The best studied process of SNARE-independent intracellular membrane fusion is mitochondrial homotypic fusion. It is a highly conserved process from yeast to humans. Observations from both yeast and mammalian cells have provided insights into the mechanism, establishing that the key players are members of the large GTPase dynamin-related protein family.

1.1.3.1 SNAREs

SNAREs (SNAP receptors) have been identified in a search for membrane receptors that bind SNAPs (soluble NSF attachment proteins) and NSF (N-ethylmaleimide sensitive factor) (Sollner *et al.*, 1993b). SNAREs constitute a compartment-specific protein family with 36 members in *Homo sapiens*. Most SNAREs are small type II membrane proteins that have tipically 20 to 30% protein similarity as a superfamily. The majority of the protein is exposed in the cytoplasm, followed by a single membrane-spanning region and a few amino acids facing either the lumen of an intracellular compartment or the extracellular side. Some SNAREs lack a membrane-spanning region, but are attached to the membrane by post-translational acyl-modifications such as palmitoylation or farnesylation. According to their function, SNAREs have been classified as v- and t-SNAREs, because they operate on opposing membranes, usually on a transport vesicle and a target membrane. Distinct trafficking steps employ different v-/t-SNARE complexes. Thus, the intracellular distribution of SNAREs provides a roadmap for membrane trafficking (Jahn *et al.*, 2006).

The structure of SNARE proteins and the architecture of SNARE complexes illustrate their mechanism. SNAREs are characterized by sequences called SNARE motifs, stretches of 60 – 70 amino acids containing heptad repeats that have a high propensity to form coiled coils; individual SNARE proteins are unfolded, but they spontaneously assemble into a remarkably stable four-helix bundle (Antonin *et al.*, 2002) that forms between membranes as a “trans-SNARE complex” (also known as a “SNAREpin”). The assembly forces membranes closely together as the complex zippers up and drives membrane fusion (Fig. 1). The reconstitution of SNAREs into liposomes has shown that cognate v- and t-SNAREs are sufficient to fuse artificial lipid bilayers (liposomes) without an additional input of energy (Weber *et al.*, 1998). Each SNAREpin releases about 35 k_BT of energy (equivalent to about 20 kcal/mol) as it zippers up. The activation energy for lipid bilayer fusion is in the range of 50 to 100 k_BT, and so three or more individual SNAREpins suitably arranged would provide enough energy to drive fusion, in line with current estimates (Hua and Scheller, 2001). However,

the number of SNAREpins actually needed to completely fuse membranes *in vivo* is not known. The membrane curvature, the lipid/protein composition of a compartment, and the presence of lipid bilayer-pertubing regulators could significantly influence the minimal number of required SNAREpins. In the postfusion state, the fully zippered SNARE complex (emanating from the fused membrane) is termed the "cis-SNARE complex."

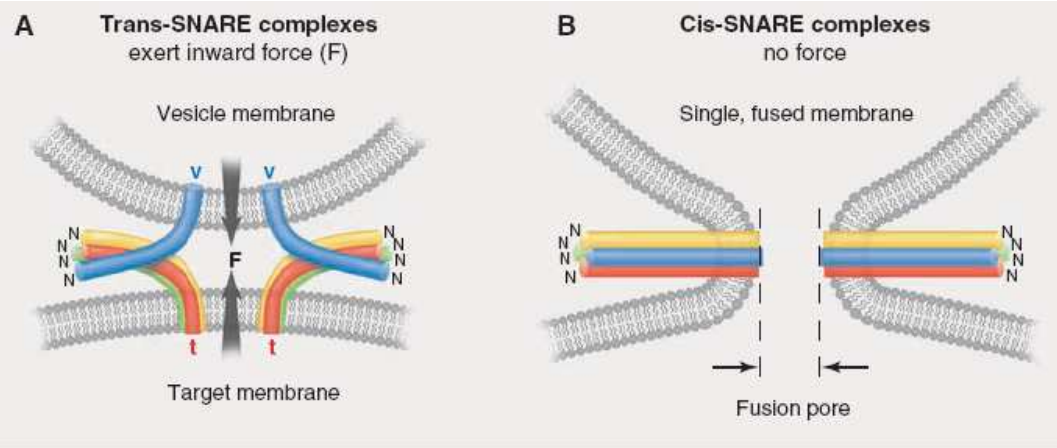

Figure 1. SNAREs mediated membrane fusion. (a) The zippering model for SNARE-catalyzed membrane fusion. Three helices anchored in one membrane (the t-SNARE) assemble with the fourth helix anchored in the other membrane (v-SNARE) to form trans-SNARE complexes, or SNAREpins. Assembly proceeds progressively from the membrane-distal N termini toward the membrane-proximal C termini of the SNAREs. This generates an inward force vector (F) that pulls the bilayers together, forcing them to fuse. Complete zippering is sterically prevented until fusion occurs, so that fusion and the completion of zippering are thermodynamically coupled. **(b)** Therefore, when fusion has occurred, the force vanishes and the SNAREs are in the low-energy cis-SNARE complex. (Südhof *et al.*, 2009)

Current evidence suggests that SNARE complex formation promotes membrane fusion by simple mechanical force, because their normal polypeptide membrane anchors can be replaced by passive lipid structures that span both leaflets. For fusion to occur, the four-helix bundle assembly has to be coupled to the transmembrane region (TM) (McNew *et al.*, 2000). Moreover, the insertion of linkers between the SNARE motif and the TM reduces or abolishes fusion *in vitro* and *in vivo* (McNew *et al.*, 1999). These data demonstrate that the linker region between the SNARE motif and the transmembrane region is critical as a force

transducer that translates the energy released upon trans-SNARE complex zippering into a catalytic force that fuses the apposing bilayers.

SNARE reconstitution into liposomes has shown that at most transport steps SNAREs function in a topologically restricted manner. Such topological restriction could significantly restrain the fusion potential of compartments and requires high accuracy in SNARE sorting. Indeed, SNAREs contribute remarkable specificity to membrane trafficking. In addition, different t-SNARE complexes with distinct v-SNARE specificities can share a common t-SNARE component. Thus, it is not necessary to encode for each transport step an entire new set of four SNAREs, and cells seem to make use of a combinatorial SNARE code. The presence of a common SNARE in different transport steps could also help to coordinate the overall membrane flow. The presence of regulatory components steers t-SNARE assembly towards functional complexes that can form fusogenic SNAREpins. Thus, in addition to the SNARE motif, many SNAREs contain an N-terminal regulatory domain. These domains adapt SNAREs to the specific needs required at the distinct transport steps. Thus, in addition to SNARE sorting, N-terminal extensions function as regulatory domains. The binding of an appropriate regulator can locally regulate SNARE function and membrane fusion (Malsam *et al.*, 2008).

SNARE complex dissociation by NSF and SNAP

Fusion is driven by an adenosine triphosphate (ATP)–dependent cycle of SNARE association and dissociation. In this cycle, the bilayer merger is thermodynamically coupled to exergonic folding of SNARE proteins, followed by their endergonic unfolding mediated by a molecular machinery that dissociates the extremely stable cis v-/t-SNARE complexes residing in a single lipid bilayer. This machinery is composed by the ATPase NSF and its adaptor protein, SNAP, the latter binding directly to the SNARE complex. When the N-terminal domain of NSF binds the SNAP/SNARE complex, ATP-hydrolysis by NSF dissociates the SNAP-SNARE complex and the four-helix SNARE bundle (Sollner *et al.*, 1993a). The resulting individual SNAREs are largely unfolded and in an energy-rich state

for another round of fusion. NSF presumably uses three to six ATPs with each catalytic cycle (totaling about 20 to 40 kcal/mol) to disrupt the SNARE complex. ATP-hydrolysis by NSF is the only step where a net input of energy is invested, in fact the actual fusion process is driven by the SNARE folding. The mechanisms that prevent the immediate reassembly of cis-SNARE complexes are not understood in detail. The N-terminal regulatory domains of SNAREs, regulatory proteins, or the sequestration/packing of the v-SNARE into transport vesicles could be potential mechanisms. In contrast to cis-SNARE complexes, SNAREpins are not substrates for NSF and SNAPs, allowing the stable formation of SNAREpin intermediates (Weber *et al.*, 2000).

Locally restricted fusion

To target vesicle fusion to distinct membrane subdomains, vesicle tethering is locally restricted. Tethering proteins can directly interact with SNAREs and provide an additional layer of specificity and contribute to high-fidelity fusion. Vesicle tethering precedes SNARE complex formation, and at least some tethering proteins play an active role in SNARE complex formation (Shorter *et al.*, 2002). Tethering factors have been identified in nearly all intracellular membrane transport steps and employ Rab proteins and some of their effectors (Grosshans *et al.*, 2006). In general, Rabs and their tethering effectors provide the local environment for efficient membrane fusion. In the presence of cognate tethering proteins, Rabs directly link membranes that subsequently undergo homo- or heterotypic fusion (Cai *et al.*, 2007).

Rabs are small compartment-specific GTPases that continuously cycle between the cytosol (in an inactive GDP-bound state) and membranes (in an active GTPbound state). Eleven Rabs have been identified in yeast, and at least 66 isoforms are expressed in mammalian cells. Membrane binding of an activated Rab protein at distinct intracellular compartments is followed by the recruitment of effectors and is temporally restricted due to GTP-hydrolysis. Rabs recruit many functional diverse effectors that operate in cargo sorting, vesicle motility, modeling of membrane subdomains, regulation of SNARE activity, or tethering.

Hence, in an orchestrated manner with their effectors, Rabs appear to coordinate the sequential steps in distinct intracellular trafficking pathways.

In contrast to highly conserved SNAREs, tethering proteins are much more heterogeneous and fall into two broad categories as long coiled-coil proteins and multisubunit complexes (Sztul and Lupashin, 2006). This suggests that tether proteins are adapted to the specific needs of the particular transport step.

In summary, tethers establish a physical link between transport vesicles and their specific target membranes and provide at least a kinetic advantage for subsequent SNAREpin assembly. The SNARE-independent sorting of tethers to membrane subdomains contributes an additional layer of vesicle targeting specificity. Some tethers directly bind specific t-SNARE components, thereby preselecting the cognate t-SNARE partner for a tethered vesicle, which might be important in the highly dynamic secretory and endocytic pathway, and at the plasma membrane where different SNAREs could exist in overlapping distributions. Many tethers are part of larger protein scaffolds harboring regulatory components that can direct vesicle trafficking, influence cytoskeleton dynamics, and more importantly could control SNARE assembly.

1.1.3.2 Dynamin-related proteins

The fundamental function of the large GTPase dynamin-related protein family is to regulate membrane dynamics in a variety of different cellular processes. The canonical member of the dynamin-related protein family, dynamin, and the mitochondrial division dynamin, Dlp/Dnm1, have been the most extensively characterized and each likely promotes membrane scission by the use of forces generated by GTPase cycle dependent self-assembly (Niemann *et al.*, 2001). Other members of the dynamin family are involved in different types of membrane remodeling events. Two of these are Mitofusins (Mfns/Fzo1) and Opa1/Mgm1, highly conserved mitochondrial dynamin like proteins, that are essential for outer and inner mitochondrial fusion respectively (Hoppins and Nunnari, 2009).

The minimal distinguishing architectural features that are common to all dynamins and are distinct from other GTPases are the structure of the large GTPase domain (~300 aminoacids). The GTPase domain is highly conserved and contains the four GTP-binding motifs (G1–G4) that are needed for guanine-nucleotide binding and hydrolysis. The conservation of these motifs is absolute except for the G4 motif in guanylate-binding proteins (GBPs). In addition to a GTPase domain, dynamin proteins possess other regions that are involved in oligomerization and regulation of the GTPase activity. These regions are often referred to as the middle domain and the GTPase effector domain (GED), although whether these regions actually form discreet structural domains is uncertain (Muhlberg *et al.*, 1997).

While other G-proteins involved in signal transduction require factors to regulate the GTPase cycle, dynamin related proteins are built to transition through the GTP hydrolysis cycle by virtue of their intrinsic structural attributes. First, unlike the small GTPases, which have a high affinity for GTP and therefore require nucleotide exchange factors (NEFs), dynamin superfamily members have a relatively low affinity for GTP and consequently do not require NEFs (Eccleston *et al.*, 2002). Probably the most functionally important unique feature of this protein family is their ability to self assemble. The most extensively characterized dynamin-related proteins, dynamin and Dlp/Dnm1, are dimeric, and self assembly of dimers into large oligomeric structures stimulates GTP hydrolysis, precluding the need for GTPase activating proteins. The middle and GED regions of dynamins are important for mediating the intra- and inter-molecular interactions required for self-assembly and oligomerization-dependent GTPase activity.

Although additional factors are not essential for their GTPase cycle, dynamins interact and potentially co-assemble with proteins that likely function as effectors to modulate their kinetic and structural properties. They are also often supplemented with independent domains required for membrane targeting, such as a pleckstrin-homology (PH) domain in dynamin to promote its association with lipids and a proline rich domain to promote interaction with proteins containing SH3 (SRC-homology-3) domains.

Few high-resolution structures of eucarytotic DRPs have been reported, presumably due to their conformational plasticity and selfassembly activity. One example is the dynamin-related human guanylate-binding protein (GBP1) which forms a crystallographic dimer whose interface is comprised of interactions between the two GTPase domains (Prakash *et al.*, 2000).

Mitochondrial fusion

The development of both *in vivo* and *in vitro* mitochondrial fusion assays has been essential for the analysis of the requirements and mechanism of outer and inner membrane fusion. In both assays, mitochondrial fusion is measured by content mixing of mitochondrial targeted fluorophores. The *in vivo* mitochondrial fusion assay was developed in yeast where, during mating, mitochondria from each haploid cell fuse and content mixing of distinguishable fluorophores targeted to various mitochondrial compartments indicates that mitochondrial fusion is active (Nunnari *et al.*, 1997). This assay has been recapitulated in mammalian cells by making PEG-fused polykaryons and observing mitochondrial content mixing (Legros *et al.*, 2002). More recently, the utilization of photo-activatable GFP allows for fusion rates to be observed in a single cell (Karbowski *et al.*, 2004).

Recapitulating mitochondrial fusion *in vitro* using yeast mitochondria allowed further dissection of mitochondrial fusion. These experiments have shown that GTP is required for both outer and inner membrane fusion *in vitro*: different non-hydrolyzable variants of GTP inhibit fusion indicating that both GTP binding and hydrolysis are required for mitochondrial fusion (Meeusen *et al.*, 2004).

The mitochondrial outer membrane fusion protein Mitofusin1 possesses coiled-coil regions that likely correspond to middle and GED regions, which have been shown to be important for inter-molecular interactions. Two bona fide transmembrane domains mediate the membrane association of the Mfns/Fzo1 family. The membrane topology of Mfns/Fzo1 places the GTPase and coiled-coil regions in the cytosol with only a short loop between the transmembrane domains in the intermembrane space (Rojo *et al.*, 2002) (Fig. 2a).

In contrast to Mfns/Fzo1, the inner mitochondrial membrane fusion protein Opa1/Mgm1 is more closely related to dynamin in that it contains canonical GTPase, middle and GED regions. The N-terminus of Mgm1 harbors a mitochondrial targeting signal and two regions of hydrophobicity, which are all required for targeting Opa1/Mgm1 to the mitochondrial inner membrane and intermembrane space (Olichon *et al.*, 2002).

Both GTP binding and hydrolysis by the mitochondrial fusion dynamin-related proteins are critical for the fusion of the outer and inner mitochondrial membranes, but the exact molecular role of the GTPase cycle in fusion is not completely understood. In contrast, more is known about the role of the GTPase cycle in the function of membrane division dynamins. Data suggest that in the GTP bound state, both dynamin and Dlp/Dnm1 assemble into helix-like structures with functionally specific dimensions and that these structures can constrict and tubulate spherical liposomes *in vitro* (Yoon *et al.*, 2001; Klockow *et al.*, 2002). Based on this and other observations, dynamin and Dnm1 have been proposed to function through a mechanochemical mechanism where the forces required for membrane constriction and division are provided by GTP driven self-assembly together with assembly stimulated GTP hydrolysis.

If the structural and kinetic properties of dynamin and Dlp/Dnm1 are shared amongst all dynamin-related proteins, this raises the question of how they are harnessed to promote membrane tethering and fusion events. Data indicate that membrane tethering is accomplished via the self-assembly of the mitochondrial fusion proteins in trans across two lipid bilayers. When tested *in vitro*, Mfn1 and to a lesser extent Mfn2, can establish interactions in trans effectively tethering isolated organelles (Ishihara *et al.*, 2004). Structural analysis of the C-terminal region of Mfn1 also supports a role for trans-interactions in mitochondrial tethering. This region contains a heptad repeat (HR), which is capable of forming a dimeric, anti-parallel coiled-coil structure via inter-molecular interactions. In addition, mutations in the HR domains of Mfn1 that block fusion lead to the accumulation of mitochondrial intermediates *in vivo* that appear to be tethered. In these cells, mitochondria are aggregated with uniform gaps of 160 Å between adjacent mitochondrial outer membranes, a distance that could correspond to

stalled tethered protein complexes (Koshiba *et al.*, 2004). Together, these data suggest that interactions in trans of the HR regions of Mitofusin1 are involved in the tethering of adjacent mitochondrial outer membranes (Fig. 2b). Mitochondria of Mfn1 or Mfn2 null cells are not able to fuse, demonstrating that the presence of functional Mfns on the mitochondrial membrane is essential for fusion to occur (Koshiba *et al.*, 2004). However it is not known whether Mitofusins alone are able to mediate the fusion of mitochondrial membranes.

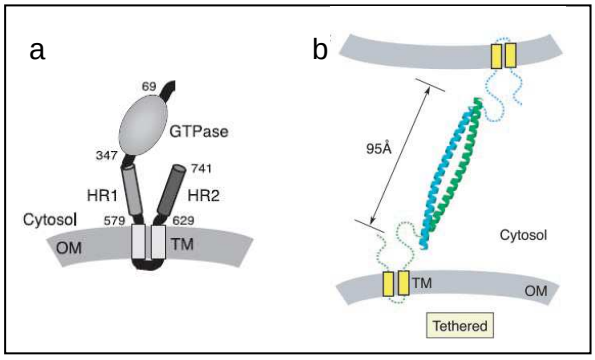

Figure 2. (a) Schematic of the Mitofusin molecule in the mitochondrial outer membrane, based on topology mapping studies. The GTPase domain, hydrophobic heptad repeats (HR), and transmembrane segments (TM) are shown. OM, mitochondrial outer membrane. **(b)** Model of the HR2 domain in a trans-Mfn1 complex in the mitochondrial outer membrane. Formation of the HR2 antiparallel coiled coil would result in tethering of adjacent mitochondria. For simplicity, the GTPase and HR1 domains are not shown (Koshiba, *et al.*, 2004).

1.2 THE ENDOPLASMIC RETICULUM

1.2.1 ER structure and organization

The endoplasmic reticulum (ER) has many different functions. These include the translocation of proteins (such as secretory proteins) across the ER membrane, the integration of proteins into the membrane, the folding and modification of proteins in the ER lumen, the synthesis of phospholipids and steroids on the cytosolic side of the ER membrane, the storage of calcium ions in the ER lumen and their regulated release into the cytosol.

The interphase ER can be divided into nuclear and peripheral ER. The nuclear ER, or nuclear envelope (NE), consists of two sheets of membranes with a

lumen. The NE surrounds the nucleus, with the inner and outer membranes connecting only at the nuclear pores, and is underlaid by a network of lamins. The peripheral ER is a network of interconnected tubules that extends throughout the cell cytoplasm. The lumenal space of the peripheral ER is continuous with that of the nuclear envelope and together they can comprise >10% of the total cell volume (Terasaki and Jaffe, 1991) (Fig. 3a).

The ultrastructure of the ER has been visualized by electron microscopy in a number of cell types. The most obvious difference seen is between rough, i.e. ribosome-studded, and smooth regions of the ER (RER and SER, respectively). The RER often has a tubular appearance, whereas the SER is often more dilated and convoluted (Baumann and Walz, 2001) (Fig. 3b). The relative abundance of RER and SER found among different cell types correlates with their functions. For example, cells that secrete a large percentage of their synthesized proteins contain mostly RER.

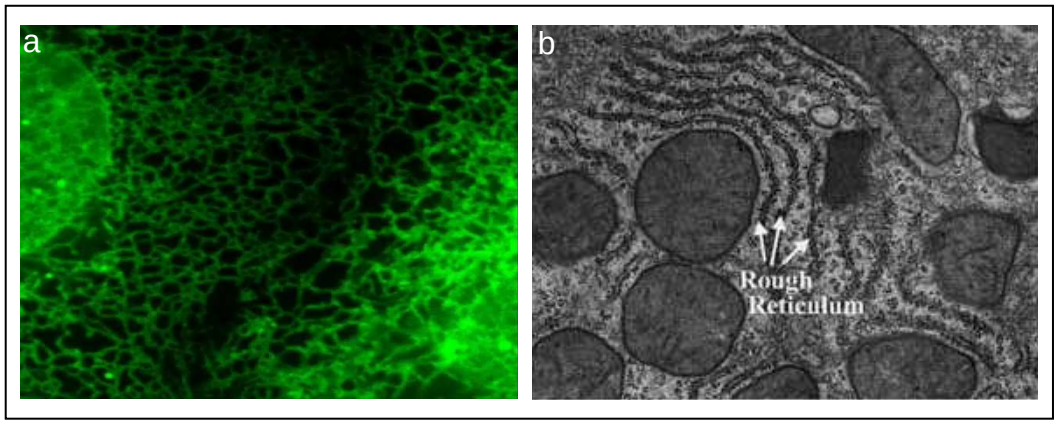

Figure 3. Ultrastructure of the ER. (a) Human osteosarcoma cells (U2OS) expressing enhanced yellow fluorescence protein (EYFP) targeted to the endoplasmic reticulum with calreticulin. **(b)** An electron micrograph of a liver cell shows RER (rough reticulum) and patches of SER (smooth reticulum). (Fawcett *et al.*, 1966)

1.2.2 The ER is a single compartment

Several approaches have provided evidence that the ER is a single membrane system with a continuous intralumenal space. In one experiment, a fluorescent dye

that cannot exchange between discontinuous membranes was injected into cells in an oil droplet. The dye diffused throughout the cell in a membrane network that, based on morphological criteria, was the ER. This was observed in a number of different cell types including sea urchin eggs (Terasaki and Jaffe, 1991) and Purkinje neurons (Terasaki *et al.*, 1994). Because the dye spread in fixed as well as live cells it must be diffusing through a continuous network rather than being transported by active trafficking.

The continuity of ER membranes network was also proved by fluorescence loss in photobleaching (FLIP). In this experiments, GFP-tagged proteins are targeted either to the lumen or membrane of the organelle, and then a small region of the labeled membrane is continuously bleached using the beam from a confocal laser scanning microscope. If membranes are interconnected, unbleached fluorescent molecules diffuse into the illuminated spot, where they are bleached; eventually, the fluorescence of the entire organelle is depleted. When FLIP experiments were performed on ER membranes, all fluorescence was rapidly lost from the entire membrane network (Dayel and Verkman, 1999), indicating the continuity of the ER membrane system.

1.2.3 Propagation of the ER during cell division

All components of the cell are dramatically rearranged during cell division. Accumulating evidence suggests that the ER network does not disassemble into vesicles during the cell cycle, but that it is divided between daughter cells by cytokinesis. The strongest support for maintenance of ER continuity comes from FLIP experiments demonstrating that ER markers retain interphase patterns of motility during mitosis (Ellenberg *et al.*, 1997). In addition, both light and electron microscopy show that ER networks can be visualized during cell division (Koch and Booth, 1988; Ellenberg *et al.*, 1997; Terasaki, 2000).

The NE disassembles during mitosis in most eukaryotic cells: the scaffolds to which NE membrane proteins are bound in interphase are reorganized, the lamina is disassembled and the chromatin is condensed. In addition,

phosphorylation of many NE proteins reduces their affinity for these partners and imaging of these proteins suggests that once freed, they diffuse throughout the ER network (Collas and Courvalin, 2000). However, biochemical fractionation of mitotic or meiotic cells has shown that vesicles are enriched in NE proteins, particularly in egg cells (Gant and Wilson, 1997). It is not clear whether this result reflects a portion of the ER that maintains a distinct composition because it is not part of the bulk ER network, or whether domains are somehow retained in the absence of scaffolds like the lamina.

1.2.4 ER dynamics

In interphase cells, the peripheral ER is a dynamic network consisting of cisternal sheets, linear tubules, polygonal reticulum and three-way junctions (Allan and Vale, 1991). Several basic movements contribute to its dynamics: elongation and retraction of tubules, tubule branching, sliding of tubule junctions and the disappearance of polygons. These movements are constantly rearranging the ER network while maintaining its characteristic structure.

The dynamics of the ER network depend on the cytoskeleton. In mammalian tissue culture cells, goldfish scale cells, and *Xenopus* and sea urchin embryos the ER tubules often co-align with microtubules. Microtubule-based ER dynamics were studied with time-lapse microscopy and appear to be based on three different mechanisms. First, new ER tubules can be pulled out of existing tubules by motor proteins migrating along microtubules. Secondly, new tubules may be dragged along by the tips of polymerizing microtubules. Finally, ER tubules may associate with the sides of microtubules, via motor proteins, as they slide along other microtubules. Each of these mechanisms can lead to tubule extension and, when tubules intersect, they fuse and create three-way junctions (Allan and Vale, 1991; Waterman-Storer and Salmon, 1998). In yeast and plants, the actin cytoskeleton, rather than the microtubule network, is required for ER dynamics (Prinz *et al.*, 2000).

The cytoskeleton contributes to ER dynamics, but it is not necessary for the maintenance of the existing ER network. Although depolymerization of microtubules by nocodazole in mammalian tissue culture cells inhibits new tubule growth and causes some retraction of ER tubules from the cell periphery, the basic tubular-cisternal structure of the ER remains intact (Terasaki *et al.,* 1986). Similarly, actin depolymerization in yeast blocks ER movements but does not disrupt its structure (Prinz *et al.,* 2000).

1.2.5 Formation and maintenance of ER network

Little is known about how the particular architecture of the ER is formed and maintained. It is known that the cytoskeleton is not necessary for the formation of a tubular network *in vitro*. In *Xenopus* egg extracts, ER networks can form *de novo* and this process is not affected by the addition of inhibitors of microtubule polymerization, by the depletion of tubulin from the extract or by inhibitors of actin polymerization (Dreier and Rapoport, 2000).

In contrast, homotypic membrane fusion is essential for preserving the typical structure of the ER (Vedrenne and Hauri, 2006), and its failure prevents the formation of an intact ER network (Dreier and Rapoport, 2000). Homotypic fusion of ER membranes depends categorically on GTP hydrolysis and does not require cytosolic proteins or ATP (Dreier and Rapoport, 2000; Voeltz *et al.*, 2006), suggesting the involvement of a GTP-dependent fusion machinery tightly associated with the ER membrane. Inhibition of network formation by GTPγS and N-ethylmaleimide (NEM) (Allan and Vale, 1991; Dreier and Rapoport, 2000), suggests that a GTPase and/or a factor similar to the NEM-sensitive fusion protein (NSF) may be involved. There is some evidence that a homolog of NSF, p97, and its co-factor p47, contribute to efficient ER network formation in *Xenopus* egg extracts (Hetzer *et al.*, 2001), and the yeast homolog of p97, Cdc48, has been shown to be involved in homotypic ER fusion (Latterich *et al.*, 1995). A role for p97/p47 in the *in vitro* formation of the transitional ER has also been suggested (Roy *et al.*, 2000). Surprisingly, however, a mutant of Cdc48 does not affect ER structure in yeast (Prinz *et al.*, 2000). The involvement of these proteins in ER

membrane fusion is indirect and neither exhibits GTPase function. Thus, the molecular components of the GTP-dependent activity responsible for homotypic fusion of ER membranes have not yet been identified.

1.2.6 Tubulation of ER membranes

Membrane tubules are a structural feature of both the ER and the Golgi complex (Lee *et al.*, 1989; Dreier and Rapoport, 2000). Both types of tubule have similar diameters (50–100 nm), whether formed *in vitro* or *in vivo*, and in the case of the ER, tubule diameter is conserved from yeast to mammalian cells, suggesting that their formation is a regulated and fundamental process.

The mechanism behind tubulation is unclear. One idea is that membrane tubules are generated by being pulled out by molecular motors as they move along microtubule or actin filaments or by the tips of filaments as these grow by polymerization, although the *in vitro* experiments do not support a role for the cytoskeleton (Dreier and Rapoport, 2000). Other models of ER network formation and maintenance postulate the existence of abundant scaffolding proteins inside or outside of the ER. However, scaffolds are not obvious in electron microscopy pictures and would be difficult to reconcile with the dynamic nature of the ER tubules, and the ER membrane is permeable to small molecules. Regulation of lumenal volume by ion pumps and water flow restriction (Voeltz *et al.*, 2002) have also been proposed to contribute to tubule shape. If lumenal volume is restricted during vesicle fusion, the shape that the fused membrane could adopt would also be restricted. For example, a sphere has a different ratio of surface area to volume than a tubule. The most obvious way to control lumenal volume would be with an ion pump to maintain an ion gradient, resulting in expulsion of solution from the lumen; however, no such mechanism has been identified.

Perhaps the most plausible models for tubule formation and maintenance are based on mechanisms that generate or stabilize high curvature in membranes. Tubules have a unique curvature of the lipid bilayer. For example, modifications that change the ratio of cone-shaped to inverted cone-shaped phospholipids in one

leaflet of the membrane bilayer relative to the other leaflet will alter membrane curvature. Proteins would be required to keep the lipid imbalance or to create curvature on their own. Two class of proteins are necessary for the generation of tubular ER: the reticulons and DP1/Yop1p. They have been proposed to be involved in stabilization of high curvature membranes by means of the hairpin formed inside the membrane by the two hydrophobic segments in these proteins (Voeltz *et al.*, 2006).

1.3 ATLASTIN

1.3.1 SPG3A

The SPG3A gene is localized on chromosome 14 and encodes a 558 amino acid protein named atlastin-1. Mutations in the SPG3A gene were identified for the first time in 2001 in Hereditary Spastic Paraplegia (HSP) patients (Zhao *et al.*, 2001). HSP are a large group of genetically heterogeneous disorders in which the main feature is the progressive spasticity in the lower limbs resulting from a 'dying back' degeneration of the cortico-spinal tracts. Among genetic forms of the disease, spasticity in the lower limbs alone is described as 'pure' HSP. Autosomal dominant is the main mode of inheritance, accounting for about 70–80% of all HSPs, and is predominantly associated with pure forms. Mutations in SPG3A gene cause the most frequent autosomal dominant form of pure HSP with very early onset and the second most frequent of all autosomal dominant forms of this disease, accounting for approximately 10% of cases (Namekawa *et al.*, 2006).

Atlastin-1 protein contains an N-terminal GTPase domain with the four conserved GTP-binding motifs (Praefcke and McMahon, 2004). Based on the high similarity of the GTPase domain, atlastin-1 has been included in the dynamin family of large GTPases. Of the members of the dynamin superfamily, atlastin-1 is most similar to GBPs. After the GTPase domain the protein presents a mid-portion, two transmembrane (TM) domains and a short C-terminal tail. Subcellular fractionation and protease protection assays revealed that atlastin-1 is an integral membrane protein with both the N-terminal GTP-binding domain and

the C-terminal region exposed to the cytoplasm (Zhu *et al.*, 2003) (Fig. 4). This structure is not typical of GBPs, that are not integral membrane proteins. Moreover, unlike atlastins, GBPs have an additional C-terminal alpha-helical domain that folds back to interact with more proximal areas (Prakash *et al.*, 2000). In this regard, the atlastins are more reminiscent of the Fzo/mitofusins, other large GTPases members of the dynamin superfamily spanning the outer mitochondrial membrane twice with both N and C termini facing the cytoplasm, that are critical for proper mitochondrial fusion (Koshiba *et al.*, 2004).

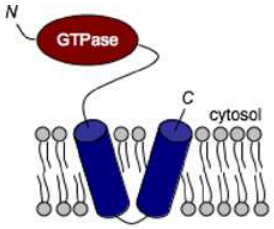

Figure 4. Membrane topology of atlastin-1 GTPase. Atlastin-1 is an integral membrane protein with both the N- and the C-terminal regions exposed to the cytoplasm.

Yeast two-hybrid analyses and co-immunoprecipitation studies demonstrated that atlastin-1 can self associate, like many members of the dynamin superfamily. Chemical cross-linking studies suggested that atlastin-1 exists as an oligomer *in vivo* but it is unclear if it forms dimeric or tetrameric structures. It is also unclear whether atlastin-1 is able to form higher order structures, as has been shown for other members of the dynamin superfamily (Zhu *et al.*, 2003).

1.3.2 Atlastin subfamily

In humans there are two other atlastin family members, named atlastin-2 and -3. This division is conserved in a variety of rodents and higher mammals. However, some species such as *Drosophila melanogaster*, *Caenorhabditis elegans*, and the sea urchin express only one atlastin, indicating that the three atlastins in higher species may have at least partially overlapping functions.

Structurally atlastin-2 and atlastin-3 are highly similar to atlastin-1: they are transmembrane proteins with N- and C- terminals facing the cytoplasm and are capable of oligomerization (Rismanchi *et al.*, 2008).

1.3.3 Human Atlastins

The atlastin-1 protein is most abundant in brain, although it is also present at lower levels in other tissues, including lung, smooth muscle, adrenal gland, kidney, and testis. Within the brain, atlastin-1 is prominently enriched in the lamina V pyramidal neurons in the cerebral cortex (Zhu *et al.* 2003).

The subcellular localization of atlastin-1 is controversial: the protein has been reported to localize to either Golgi (Zhu *et al.* 2003; Namekawa *et al.* 2007) or endoplasmic reticulum membranes (Namekawa *et al.* 2007). Atlastin-1 has also been reported to be enriched in vesicular structures within axonal growth cones and varicosities as well as at axonal branch points in cultured cerebral cortical neurons (Zhu *et al.*, 2006).

Atlastin-2 and atlastin-3 are expressed at higher levels in peripheral tissues and much less in the brain (Zhu *et al.*, 2003; Rismanchi *et al.*, 2008). At the subcellular level, atlastin-2 and atlastin-3 show prominent localization to the endoplasmic reticulum (Rismanchi *et al.*, 2008).

Studies in rat cortical neurons showed that knock-down of atlastin-1 resulted in the inhibition of axon formation and elongation suggesting a possible role of atlastin-1 in neurite outgrowth during neuronal development (Zhu *et al.*, 2006). Atlastin-1 has been proposed to be implicated in vesicle trafficking at the ER/Golgi interface and in the maturation of the Golgi complex. Expression in HEK293 cell cultures of atlastin-1 GTPase deficient mutants appeared to interfere with the maturation of Golgi complexes by preventing the budding of vesicles from the endoplasmic reticulum (Namekawa *et al.* 2007).

Atlastin family members have been also proposed to be required for endoplasmic reticulum and Golgi apparatus morphogenesis. Expression in HeLa cells of mutant or dominant-negative forms of atlastin-1, -2 or -3 that lack GTPase

activity resulted in prominent changes in ER morphology, with loss of typical reticularization, suggesting a role for atlastin GTPases in the formation of three-way junctions in the ER. Overexpression of wild type atlastin-1, -2 or -3 did not cause the same morphologichal change in ER morphology, while it resulted in fragmentation of the Golgi structure into “mini stacks”. Knockdown of atlastin-2 and -3 levels in cells using siRNA caused abnormalities in Golgi morphology, most commonly fragmentation. Expression of wild type and dominant-negative atlastins and siRNA knockdown studies revealed essentially normal ER-to-Golgi trafficking. These data suggested a possible role of atlastins in both Golgi and Endoplasmic reticulum morphogenesis, but they do not appear to be required for ER-to-Golgi trafficking (Rismanchi *et al.*, 2008).

1.3.4 Drosophila atlastin (Datlastin)

A single ortholog of mammalian atlastins exists in *Drosophila*. It maps to the 96A13 band of the third chromosome and encodes a 541 aminoacid protein named Datlastin. *Drosophila* atlastin protein inspection reveals an extensive homology, with 56% of identity and 77% of similarity, with human atlastin-1.

A *Drosophila* line containing a null mutation in Datlastin gene named atl^1 has been isolated (Lee *et al.* 2006). The homozygote atl^1 flies were viable but sterile and were smaller in body size than wild-type. Moreover, atl^1 flies had a very short life span, approximately 50-60% shorter than wild-type control flies. Loss of Datlastin was shown to give rise to age dependent motor dysfunctions. This phenotype was associated with a progressive degeneration of dopaminergic neurons as the flies aged, suggesting that the mechanisms of human HSP symptoms resulting from atlastin-1 mutation could be the degeneration of dopaminergic neurons (Lee *et al.* 2006).

In the neuromuscular system loss of Datlastin led to abnormal growth of the muscle and neuromuscular junction, suggesting that Datlastin could have a role in synapse development. Moreover, defects in ER and Golgi morphogenesis have been reported (Lee et al, 2009).

1.4 *DROSOPHILA* AS A MODEL ORGANISM

Ever since Morgan isolated the *white* mutation in *Drosophila melanogaster* in 1910, the tiny fruit fly has made large contributions to the understanding of the genetic and molecular mechanisms of heredity and development. More recently, the remarkable power of fruit fly genetics has been applied to study the basic mechanisms of human diseases, including those debilitating pathologies that affect the human brain.

There are several reasons why *D. melanogaster* is widely used as models of human diseases (Bier, 2005). The first and foremost reason is based on the presumption that fundamental aspects of cell biology in flies have been conserved throughout evolution in higher-order organisms such as humans. A report demonstrating that approximately 75% of the disease-related loci in humans have at least one *Drosophila* homologue confirms the high degree of conservation present in flies (Reiter *et al.*, 2001). Furthermore, studies of developmental events in the fly and subsequent similar studies in higher animals have revealed a stunning degree of functional conservation of genes. These studies indicate that not only basic cell biology but also higher-order events such as organ 'construction' and function are conserved.

Apart from the genetic similarities between the fruit fly and humans, fundamental similarities in their brains are also apparent. Although morphologically distinct and of lower complexity, the *D. melanogaster* CNS comprises the same basic building blocks as the mammalian CNS. The fly brain is estimated to have, strikingly enough, in excess of 300,000 neurons and similarly to mammals is organised into areas with separated specialised functions such as learning, memory, olfaction and vision. Neurons and glial cells form the main constituents, and many of their characteristics, such as the neurotransmitter systems, are conserved (Thor, 1995) (Fig. 5). These properties, apart from making the fruit fly a good model in neurobiological research, make *D. melanogaster* a powerful tool for the understanding of the genetic and molecular mechanisms of neural development and for the investigation of the neural basis of behaviour. Taking advantage of the powerful genetic tools offered by the fruit fly,

the organization of the neural circuitry that underlies olfactory perception, sexual behaviour and circadian rhythmicity are also being unravelled. (Celotto and Palladino, 2005; Cauchi and van den Heuvel, 2006)

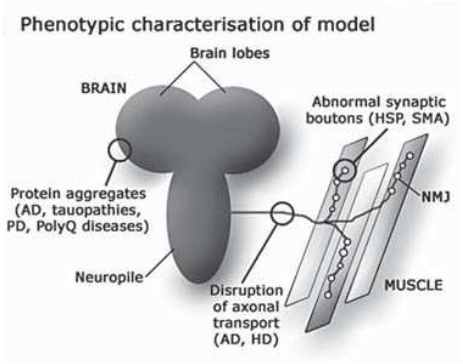

Figure 5. The nervous system of vertebrates and invertebrates is very similar. A schematic of the larval brain is shown here. Motor neurons project from the neuropile (equivalent to the vertebral column in vertebrates) towards muscles where they form neuromuscular junctions (NMJs). Because the fly nervous system is well characterised and highly accessible, its phenotypic analysis is undemanding. HD = Huntington disease; HSP = hereditary spastic paraplegia. (Cauchi, van den Heuvel, 2006)

D. melanogaster has the practical advantages of being small, highly fertile and having a short generation time with large progeny numbers. These characteristics allow large-scale experiments, such as genetic screens for mutations affecting a relevant process, to be performed in a relatively short period of time and at low cost. The *D. melanogaster* genome is small, fully sequenced and annotated and devoid of genetic redundancy, and is publicly available (www.flybase.org). *Drosophila* has an unrivalled battery of genetic tools including a rapidly expanding collection of mutants, transposon-based methods for gene manipulation, systems that allow controlled ectopic gene expression and balancer chromosomes. These genetic-transformation techniques provide a flexible tool for genetic studies of the molecular pathways underlying a biological process of interest (Venken & Bellen, 2005).

Flies also provide a platform for rapid drug discovery because it is easy to generate large numbers of genetically identical animals that can be tested in drug

screens. Such work is prone to contribute to the identification of novel hits in the lengthy pharmaceutical pipeline.

2. METHODS

2.1 Molecular biology

The Datlastin full-length complementary DNA was previously obtained by RT–PCR performed on total *Drosophila* head RNA. The cDNA was cloned in pDrive vector (Qiagen).

2.1.1 Introduction of K51A substitution in Datlastin cDNA

To introduce the nucleotide substitutions K51A in Datlastin cDNA, site-directed mutagenesis was performed using Pfu Ultra HF DNA polymerase (Startagene). The basic procedure utilizes a supercoiled double-stranded DNA (dsDNA) vector with an insert of interest and two synthetic oligonucleotide primers containing the desired mutation. The oligonucleotide primers, each complementary to opposite strands of the vector, are extended during temperature cycling by the Pfu Ultra DNA polymerase. Pfu Ultra DNA polymerase replicates both plasmid strands with high fidelity and without displacing the mutant oligonucleotide primers. Incorporation of the oligonucleotide primers generates a mutated plasmid containing staggered nicks. Following temperature cycling, the product is treated with DpnI. The DpnI endonuclease (target sequence: 5´-Gm6ATC-3´) is specific for methylated and hemimethylated DNA and is used to digest the parental DNA template to select for mutation-containing synthesized DNA. DNA isolated from almost all *E. coli* strains is methylated and therefore susceptible to DpnI digestion. The nicked vector DNA containing the desired mutations is then transformed into XL1-Blue chemiocompetent cells.

To generate the substitution of a Lysine in an Alanine in position 51 of Datlastin cDNA, the following primers were used:

Datl K51A F 5’TTCCGAAAGGGCGCGAGCTTCCTGCTG3’

Datl K51A R 5’CAGCAGGAAGCTCGCGCCCTTTCGGAA3’

PCR reaction

10X PfuUltra HF reaction buffer	5 ul
Datlastin/pDRIVE	50 ng
Forward primer (10 uM)	2 ul
Reverse primer (10 uM)	2 ul
10 mM dNTPs	1 ul
Pfu Ultra HF DNA polymerase	2.5U
H_2O	to 50 ul

PCR cycle

95°C	1 minute	
95°C	50 seconds	18 cycles
52°C	50 seconds	
68°C	10 minutes	
68°C	30 minutes	

Following temperature cycling, the reaction was placed on ice.

10U of the DpnI restriction enzyme were added directly to the amplification. The reaction was mixed by pipetting the solution up and down several times, and immediately incubated at 37°C for 1 hour to digest the parental (i.e., non mutated) supercoiled dsDNA.

Transformation

10 μl of the reaction mixture was used for transformation of chemically competent DH5alpha cells (Invitogen). Transformed bacteria were plated on LB–ampicillin agar plates and incubated overnight at 37°C.

10 colonies were grown in LB medium with ampicillin. Plasmid DNA was successively purified by minipreparation protocol (Appendix A).

Plasmid purification

The presence of the mutation was verified by sequencing.

Datl K51A/pDRIVE plasmid was purified from an overnight culture using a "Midi" plasmid purification kit, according to Qiagen Plasmid Midi purification protocols. The final pellet was re-suspended in 50 ul of TE buffer.

2.1.2 Cloning of wild type and mutated Datlastin cDNA in pcDNA3 Zeo+ plasmid

pcDNA3.1/Zeo(+) is a plasmid designed for high level expression in a variety of mammalian cell lines (Appendix C).

Two differently tagged versions of wild type and mutated Datlastin were cloned in the pcDNA3.1/Zeo(+) plasmid, generating the following constructs:

Datlastin-HA/pcDNA3.1 Zeo(+)

Datlastin-Myc/pcDNA3.1 Zeo(+)

Datlastin^{K51A}-HA/pcDNA3.1 Zeo(+)

Datlastin^{K51A}-Myc/pcDNA3.1 Zeo(+)

To insert the HA epitope in the C-terminus of Datlastin, cDNA was amplified from Datlastin/pDrive or Datlastin^{K51A}/pDrive vector using the following primers:

AtlATGEcoRI F	5'AGCTGAATTCATGGGCGGATCGGCAGTGCAGG3'
THM XhoI HA R	5'AGCTCTCGAGCTAGCCCGCATAGTCAGGAACATC GTATGGGTATGACCGCTTCACCTTGCCATTG3'

To insert the Myc epitope in the C-terminus of Datlastin, cDNA was amplified from Datlastin/pDrive or Datlastin^{K51A}/pDrive vector using the following primers:

AtlATGEcoRI F	5'AGCTGAATTCATGGGCGGATGGGCAGTGCAGG3'
THM XhoI Myc R	5'AGCTCTCGAGCTACAGATCTTCTTCAGAAATAAGT TTTTGTTCTGACCGCTTCACCTTGCCATTG3'

PCR reaction

5X Phusion HF buffer	10 ul
Datlastin/pDrive template	50 ng
Forward (10 uM)	2 ul
Reverse (10 uM)	2 ul
10 mM dNTPs	1 ul
Phusion DNA polymerase	2.5U
H_2O	to 50 ul

PCR cycle

98°C	30 seconds	
98°C	10 seconds	30 cycles
57°C	20 seconds	
72°C	1 minute	
72°C	10 minutes	

Restriction reactions

pcDNA3.1/Zeo(+) plasmid and PCR fragments were digested with EcoRI and XhoI restriction enzymes:

Datlastin PCR fragment	2 µg	pcDNA3.1/Zeo(+)	2 µg
EcoRI	20 U	EcoRI (10U/ul)	20 U
XhoI (10U/ul)	20 U	XhoI (10U/ul)	20 U
10X buffer	5 ul	10X buffer	5 ul
H_2O	to 50 ul	H_2O	to 50 ul

Mixed products were incubated at 37°C for 1 hour and successively separated by electrophoresis in a 1% agarose gel. The bands corresponding to the Datlastin PCR fragments and pcDNA3.1/Zeo(+) plasmid were cut from gel and purified using the QIAquick Gel Extraction Kit (Qiagen). Purified DNA products were eluted in 20 µl of elution buffer.

The purified DNA fragments were ligated as follows:

pcDNA3.1/Zeo(+)	150 ng
Datlastin fragment	300 ng
10X Ligation buffer	1 ul
T4 DNA ligase (Biolabs)	1 ul
H_2O	to 10 ul

The mixture was incubated at room temperature for 1 hour.

Transformation

Ligation mixture was used for transformation of chemically competent DH5alpha cells (Invitogen). Transformed bacteria were plated on LB–ampicillin agar plates and incubated overnight at 37°C. 10 colonies for each construct were grown in LB

medium with ampicillin. Plasmid DNA was successively purified by minipreparation protocol (Appendix A) and tested by restriction analysis.

Purification of HA and Myc tagged wild type and mutated Datlastin in pcDNA3.1/Zeo(+)

Plasmid DNA were purified from an overnight culture using a "Midi" plasmid purification kit, according to Qiagen Plasmid Midi purification protocols. The final pellets were re-suspended in 50 ul of TE buffer.

2.1.3 Cloning Datlastin^{K51A} cDNA in pUAST

pUAST plasmid (Appendix C) and Datlastin cDNA carrying the K51A mutation in pDRIVE were digested with EcoRI and XhoI restriction enzymes:

Datlastin^{K51A}/pDrive	2 µg	pUAST plasmid	2 µg
EcoRI	20 U	EcoRI	20 U
XhoI	20 U	XhoI	20 U
10X buffer	5 ul	10X buffer	5 ul
H_2O	to 50 ul	H_2O	to 50 ul

Mixed products were incubated at 37°C for 1 hour and successively separated by electrophoresis. The bands corresponding to the mutated Datlastin^{K51A} cDNA and pUAST plasmid were cut from gel and purified using the QIAquick Gel Extraction Kit (Qiagen). Purified DNA products were eluted in 20 µl of elution buffer.

The two purified DNA fragments were ligated as follows:

pUAST plasmid	150 ng
Datlastin^{K51A} cDNA fragment	300 ng
10X Ligation buffer	1 ul
T4 DNA ligase (Biolabs)	1 ul
H_2O	to 10 ul

The mixture was incubated at room temperature for 1 hour.

Transformation

Ligation mixture was used for transformation of chemically competent DH5 alpha cells (Invitogen). Transformed bacteria were plated on LB–ampicillin agar plates and incubated overnight at 37°C.

10 colonies were grown in LB medium with ampicillin. Plasmid DNA was successively purified by minipreparation protocol (Appendix A) and tested by restriction analysis.

Plasmid purification

Datlastin^{K51A}/pUAST plasmid was purified from an overnight culture using a "Midi" plasmid purification kit, according to Qiagen Plasmid Midi purification protocols. The final pellet was re-suspended in 50 ul of TE buffer.

2.2 Biochemical techniques

2.2.1 Co-Immunoprecipitation

For co-immunoprecipitation (co-IP) experiments anti-c-Myc agarose conjugate (Sigma) prepared linking an anti-c-Myc antibody developed in rabbit to an agarose support matrix was used. Anti-c-Myc antibody recognizes the c-Myc epitope allowing the isolation of Datlastin-myc and other proteins potentially

bound to it. The sample can then be separated by SDS-PAGE for Western blot analysis.

The co-immunoprecipitation protocol used is the following:

- HeLa cells were cotransfected with -HA and -Myc tagged versions of Datlastin using Lipofectamine™ 2000 Transfection Reagent (Invitrogen) following standard protocols
- 24 hours after transfection, 10^6 cells were harvested using 0.5% Triton X-100 (Applichem) in PBS, incubated in ice for 15 minutes and then centrifuged at 16000g for 15 minutes.
- 30 ul of anti-c-Myc agarose conjugate suspension (Sigma) was added to a microcentrifuge tube and washed 5 times with PBS by a short spin.
- Cell extract (lysate) was added to the resin and incubated for 2 hours on an orbital shaker at room temperature.
- At the end of incubation time, the supernatant was recovered and the resin was washed 3 times with PBS.
- After the final wash, 70 ul of 1X Laemmli buffer (see Appendix B) were added to the resin and incubated at 95°C for 5 minutes.
- After boiling, the sample was vortexed and centrifugated for 5 seconds and the supernatant was recovered (pellet).
- Lysate, supernatant and pellet were analysed by western blotting.

2.2.2 Immunoisolation of membrane vesicles and membrane fractionation

To obtain harbouring vesicles, the sample were prepared as follows:

- HeLa cells were transfected separately with -HA or -Myc tagged versions of Datlastin using Lipofectamine™ 2000 Transfection Reagent (Invitrogen) following standard protocols
- 10^6 transfected cells were suspended in homogenization buffer (10 mM HEPES-KOH buffer pH 7.4 containing 0.22 M mannitol, 0.07 M sucrose and protease inhibitors) and homogenized using a syringe with a 26-gauge needle.

- Homogenate was sonicated and the supernatant containing vesiculated membranes recovered by centrifugation at 4000g for 5 minutes at 4°C to remove unbroken organelles.
- The vesiculated membranes containing –HA and –Myc tagged Datlastin were then mixed and incubated at 30°C for 1 hour.
- After incubation, immunoprecipitation of the harbouring vesicles was performed in the absence of detergent as described above.
- The remaining supernatants containing vesiculated membranes were centrifugated at 120000 g for 60 minutes to separate a membrane fraction (pellet) and a soluble fraction (supernatant).
- Supernatant and pellet derived from the immunoprecipitation and 100000 g centrifugation were analysed by western blotting.

2.2.3 SDS PAGE

Electrophoresis

The resolving gel was prepared with 10% polyacrylamide, while the stacking gel had a 5% acrylamide concentration.

	Resolving gel	Stacking gel
Acrylamide solution (Fluka)	10% (v/v)	5% (v/v)
Tris-HCl pH 8.8	0.37M	
Tris-HCl pH 6.8		0.125M
Ammonium persulphate	0.1% (w/v)	0.1% (w/v)
SDS	0.1% (w/v)	0.1% (w/v)
TEMED	0.02% (v/v)	0.02% (v/v)

Samples were diluted in Laemli buffer (Appendix B), boiled for 5 minutes and loaded.

Western blotting

After the electrophoresis, the proteins were transferred from gel to PVDF membrane (Amersham Biosciences). The membrane was then blocked with a solution of 10% milk in TBS-T (Appendix B) for 15 minutes at room temperature on an orbital shaker and incubated with the primary antibody diluted to the appropriate concentration in TBS-T and 2% milk, at 4°C O/N. After washing the membrane with TBS-T, the secondary antibody diluted in TBS-T was added and incubated for 1 hour at room temperature. The membrane was washed and the detection was performed using the ECL plus kit (Amersham Biosciences).

2.3 *Drosophila* transformation

Fruit flies begin their lives as an embryo in an egg. This stage lasts for about one day when the embryo develops into a larva. The larval development lasts six days, then the larva stops moving and forms a pupa. During the five days in the pupal case, the metamorphosis from larva to adult occurs. When the adults emerge from the pupa they are fully formed. They become fertile after about ten hours, copulate, the females lay eggs, and the cycle begins again. The whole life cycle takes about 12-14 days.

2.3.1 Microinjection

The DatlastinK51A/pUAST plasmid was prepared for microinjection. The helper plasmid is a source of P-element transposase that allows the insertion of DNA construct into the fly genome.

Microinjection mix:

Datlastin^{K51A}/pUAST	3 μg/μl
Helper plasmid	1 μg/μl
10XMicroinjecting buffer	1X

The mix is filtered through a 0.2 μm Micro-spin Filter Tube (Alltech).

The injection set-up consists of two parts: an inverted microscope (Nikon) equipped with a 20X lens and a micromanipulator InjectMan (Eppendorf) linked to the FemtoJet air-pressure injecting device (Eppendorf) connected to the needle holder. The set-up was installed in a cool room (18˚/20°C) to slow the embryo development.

Needles were prepared on a horizontal puller (Flaming/Bown Micropipette Puller Model P 80/PC) using 1.0 mm OD borosilicate capillaries (World Precision Instruments).

The settings used for the needles preparation were:

Heat=414 Pull=200 Vel=250 Time=150

The microinjection mix was introduced in a needle that was connected to the needle holder.

w^{1118} strain was used for microinjection. These flies have white eyes, allowing the detection of the transgene insertion in the offspring. After 20 minutes of eggs laying, embryos were collected, washed briefly and transferred in a small quantity of water to the centre of a coverslip with a clean thin pointed brush. 100 moist embryos were lined up with a dissection needle near one edge of the coverslip, with the posterior pole pointing to the edge. Embryos were let to dry for a few minutes to attach them firmly to the coverslip and then covered with as little halocarbon oil mix as possible. After 5-10 min the oil has penetrated between the chorion and the vitelline membrane clearing the embryo and allowing a rough staging under the dissecting scope. Embryos must be injected before blastoderm cellularization, a developmental stage that begins 45-50 minutes after eggs are laid at 22°C. Cellularization is easily visible at the microscope, and such old embryos were not injected.

The microinjection of the embryos was completely automatic, the needle was inserted quickly in the centre of the posterior pole were the germ cells will form, and pulled out quickly to avoid any leakage. After the injection most of oil was drained off the coverslip and the embryos were gently transferred to a food vial mantained at 18-20°C until adults hatched.

2.3.2 Characterization of transgenic lines

Hatching adults (F0) were separated by sex and crossed to w^{1118} flies. The F1 offspring was screened for transformant individuals where exogenous DNA was inserted in the fly genome. Transgenic flies selected for the red eye phenotype will be crossed with "balancer" lines that carry dominant phenotypic markers to generate a stable transgenic line and avoid transgene loss.

F1 individuals may bear one transgene insertion on any of the chromosomes: X, II, III or IV. Transgenes inserted on the fourth chromosome are very rare as this chromosome is rather small and essentially heterochromatic.

Each transgenic F1 fly is crossed with the second chromosome balancer stock Sm6a/TfT, carrying the dominant morphological marker *CyO* that produces curly wings. Individuals of the F2 carrying the transgene (selected for red eyes) and the *CyO* marker (selected for curly wings) were crossed to generate a stable transgenic line.

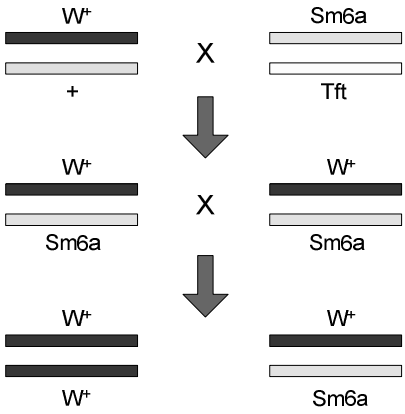

Figure 6. Cross with II chromosome balancer.

Each transgenic F1 fly is crossed with the third chromosome balancer stock TM3/TM6, carrying the dominant morphological marker *Sb* that produces stubble hairs. Individuals of the F2 carrying the transgene (selected for red eyes) and the

Sb marker (selected for stubble hairs) were crossed to generate a stable transgenic line.

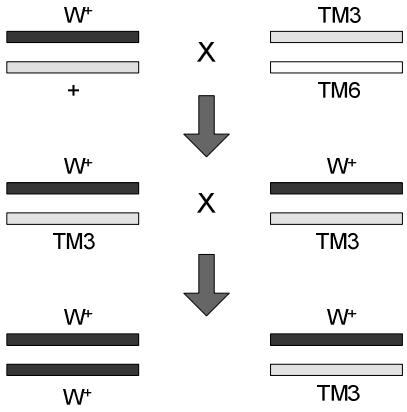

Figure 7. Cross with III chromosome balancer.

Each transgenic F1 male fly is crossed with the X chromosome balancer stock Fm7/Sno, carrying the dominant morphological marker *Bar* that produces heart-shaped eyes. If the insertion is occurred in the X chromosome, all the F1 females have heart-shaped red eyes. These female were crossed with males of the X chromosome balancer stock Fm7/Y to generate a stable transgenic line.

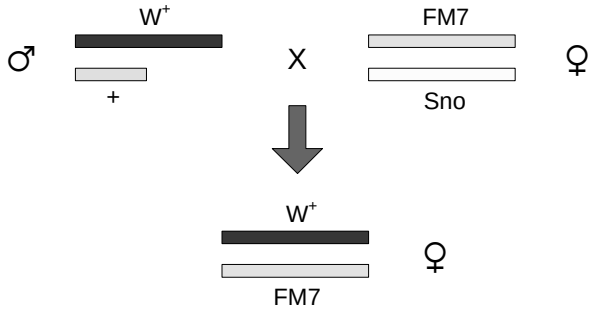

Figure 8. Cross with X chromosome balancer.

2.3.3 Drosophila genetics

Fly culture and transgenesis were performed using standard procedures. Several transgenic lines for each construct were generated and tested.

Transgenic lines for overexpression and downregulation of Datlastin were previously obtained: the Datlastin cDNA was subcloned in the pUAST vector in-frame with a Myc tag; the UAS-*Datlastin*-RNAi construct was made by introducing the entire Datlastin cDNA lacking the start codon in a Gateway-modified SympUAST vector.

Drosophila strains used: elav-Gal4, D42-Gal4, GMR-Gal4, tubulin-Gal4, nanos-Gal4:VP16, UAS-mCD8-GFP (Bloomington); UAS-aCOP-RNAi, UAS-Sar1-RNAi (VDRC); MHC-Gal4; Mef2-Gal4; armadillo-Gal4; pUASp:Lys-GFP-KDEL, pUASp:GalT-GFP and Sar1-GFP.

Control genotypes varied depending on individual experiments, but always included promoter-Gal4/+ and UAS-transgene/+ individuals.

2.4 Microscopy

2.4.1 Immunohistochemistry

Freshly collected embryos were dechorionated, devitellinized, and fixed in 4% formaldehyde in PEM buffer for 20 min before immunolabelling.

Wandering third instar larvae raised at 25°C were dissected dorsally in phosphate-buffered saline (PBS) and fixed in 4% paraformaldeyde for 20 min. Preparations were subsequently washed in PBS containing 0.3% Triton-X.

Primary antibodies were applied overnight at 4°C, secondary antibodies were incubated for approximately 2 hr at room temperature.

Antibodies

The anti-Datlastin antibody was previously produced. A synthetic peptide (VGGGAASYRSQTSVNASNGKVKRS) was used to immunize guinea pigs (BioGenes).

The following antibodies were used: mouse anti-Myc (1:500, Cell Signaling), rabbit anti-Myc (1:200, Santa Cruz Biotechnology), mouse anti-HA (1:1,000, Cell Signaling), guinea pig anti-Datlastin (1:1000), rat anti-BiP (1:50, Babraham), mouse anti-p120 (1:600, Calbiochem), mouse anti-GFP (1:500, Roche), mouse anti-Dlg (1:100, DSHB), mouse anti-PDI (1:500, Stressgen), rabbit anti-calnexin (1:1,000, Millipore). Secondary antibodies for immunofluorescence (Cy5 and Cy3 conjugates from Jackson laboratories, Alexa Fluor 488 conjugates from Invitrogen) were used at 1:1,000. Anti-mouse, anti-guinea pig and anti-rabbit HRP conjugates from DACO were used at 1:10,000.

2.4.2 Fluorescence loss in photobleaching

Experimental larvae expressing UAS-GFP-KDEL were dissected in Ca^{2+}-free HL3 and analysed using a Nikon C1 confocal microscope with a 60x water immersion objective. Two different ROI for each genotype distributed along muscle 6 or 7 in the abdominal segment 4 were selected and bleached by 20 iterations, at 100% laser power, followed by three scanning images every 15 s. The bleaching protocols were repeated for 1 h. The area of ROI in Datl-RNAi muscle was approximately 60% of the ROI area in control muscle to reflect the smaller size of Datl-RNAi larvae. To create fluorescence recovery curves, fluorescence intensities were transformed into a 0–100% scale and were plotted using Excel software. Each FLIP experiment was repeated at least three times.

2.4.3 Image analysis

Confocal images were acquired through x40 or x60 CFI Plan Apochromat Nikon objectives with a Nikon C1 confocal microscope and analysed using the NIS

Elements software (Nikon). Figure panels were assembled using Adobe Photoshop CS4.

Quantification of the mean fluorescence intensity of mCD8-GFP at the neuromuscular junction was achieved by normalizing it to the intensity of DLG antibody. For each genotype, eight neuromuscular junctions innervating muscle 4, segment A2, were imaged and statistically analysed.

P values reported in this study are two tailed values and derived from a Student's t-test, assuming unequal variances.

2.4.4 Electron microscopy

Pre-embedded gold labelling of Datlastin was done according the protocol described previously. In brief, S2 cells were fixed in 4% paraformaldehyde and 1% glutaraldehyde, washed, incubated with the anti-Datlastin antibody (1:100) overnight and then with Nanogold conjugated Fab fragments of the secondary antibodies (Nanoprobes) for 2 h. The Nanogold particles were developed using the Gold-enhance kit. Labelled cells were dehydrated, embedded in Epon, and sectioned.

Drosophila brains and larvae were fixed in 4% paraformaldehyde and 2% glutaraldehyde and embedded as described earlier.

EM images were acquired from thin sections under a Philips Tecnai-12 electron microscope using an ULTRA VIEW CCD digital camera (Soft Imaging Systems GmbH).

Quantification of anti-Datlastin labelling was done by counting gold particles in 65 cells. EM images of individual neurons for the measurement of the length of ER profiles were collected from three brains for each genotype. In total, 18 Datl-RNAi, 20 atl^{1} and 17 control neurons were analysed. In the rescue experiment a total of 26 neurons expressing wild-type Datlastin and 23 neurons expressing $Datlastin^{K51A}$ were analysed. Quantitative analyses were performed with AnalySIS software (Soft Imaging Systems GmbH).

Appendix A: General protocols

Transformation of chemiocompetent cells

- Gently thaw the chemiocompetent cells on ice.
- Add ligation mixture to 50 µl of competent cells and mix gently.
- Incubate on ice for 30 minutes.
- Heat-shock the cells for 30 seconds at 42°C without shaking.
- Immediately transfer the tube to ice.
- Add 450 µl of room temperature S.O.C. medium.
- Shake horizontally (200 rpm) at 37°C for 1 hour.
- Spread 20 µl and 100 µl from the transformation on pre-warmed selective plates and incubate overnight at 37°C.

Preparation of plasmid DNA by alkaline lysis with SDS: minipreparation

- Inoculate 3 ml of LB medium (Appendix B) containing the appropriate antibiotic with a single colony of transformed bacteria. Incubate the culture overnight at 37°C with vigorous shaking.
- Pour 1.5 ml of the culture into a microfuge tube. Centrifuge at maximum speed for 30 seconds in a microfuge. Store the unused portion of the original culture at 4°C.
- Remove the supernatant, leaving the bacterial pellet as dry as possible.
- Resuspend the bacterial pellet in 100 µl of ice-cold Alkaline lysis solution I (Appendix B) by vigorous vortexing.
- Add 200 µl of freshly prepared Alkaline lysis solution II (Appendix B) to each bacterial suspension. Mix by inverting the tube rapidly five times.
- Add 150 µl of ice-cold Alkaline lysis solution III (Appendix B 0). Close the tube and disperse Alkaline lysis solution III through the viscous bacterial lysate by inverting the tube several times. Incubate the tube on ice for 3-5 minutes.
- Centrifuge the bacterial lysate at maximum speed for 10 minutes at 4°C in

a microfuge. Transfer the supernatant to a fresh tube.

- Precipitate nucleic acids from the supernatant by adding 2 volumes of ethanol at room temperature. Mix the solution by vortexing and then allow the mixture to stand for 2 minutes at room temperature.
- Collect the precipitate of nucleic acid by centrifugation at maximum speed for 15 minutes at 4°C in a microfuge.
- Remove the supernatant by aspiration.
- Add 2 volumes of 70% ethanol to the pellet and invert several times.
- Recover the DNA pellet by centrifugation at maximum speed for 5 minutes at 4°C in a microfuge.
- Remove carefully all the ethanol by gentle aspiration.
- When the pellet is dry, dissolve the nucleic acids in 50 ul of distilled water containing 20 ug/ml DNase-free RNase A. Vortex the solution gently for a few seconds. Store the DNA solution at -20°C.

Appendix B: Stocks and solutions

LB Medium (Luria-Bertani Medium)

Bacto-tryptone	10g
Yeast extract	5g
NaCl	10g
H_2O	to 1 Liter

Autoclave.

LB Agar

Bacto-tryptone	10g
Yeast extract	5 g
NaCl	10 g
Agar	20g
H_2O	to 1 Liter

Adjust pH to 7.0 and autoclave.

LB–Ampicillin Agar

Cool 1 Liter of autoclaved LB agar to 55° and then add 100 ug/ml filter-sterilized ampicillin. Pour into petri dishes (~25 ml/100 mm plate).

SOC medium

Bacto-tryptone	20g
Yeast extract	5 g
NaCl	0,5 g
KCl 1M	2,5 ml
H_2O	to 1 Liter

Adjust pH to 7.0, autoclave and add 20 ml of sterile 1 M glucose.

Alkaline lysis solution I

Glucose 50 mM

Tris HCl 25 mM (pH 8.0)

EDTA 10 mM (pH 8.0)

Alkaline lysis solution II

NaOH 0.2 N

SDS 1%

Alkaline lysis solution III

Potassium acetate 3 M

Glacial acetic acid 11.5%

TE Buffer

Tris-HCl 10 mM (pH 7.5)

EDTA 1 mM

Phoshate Buffered Saline (PBS)

KH_2PO_4	15 g/L
NaCl	9 g/L
Na_2HPO_4	8 g/L

Running buffer 1X

Tris 25mM

Glycine 250mM

SDS 0.1%

Transfer buffer 1X

Tris 25mM

Glycine 192mM

TBS-T buffer 1X

Tris 100mM

NaCl 1,5M

Tween-20 1%

Laemmli buffer 2X

SDS 4%

Glycerol 20%

2-mercaptoethanol 10%

Bromphenol blue 0,004%

Tris HCl 125mM

10X Microinjection buffer:

Sodium Phosphate Buffer pH 6.8 0.1M

KCl 5mM

***Drosophila*'s food**

Agar	15 g
Yeast extract	46.3 g
Sucrose	46.3 g
H_2O	to 1 Liter

Autoclave and then add 2 g of Nipagine dissolved in 90% ethanol.

Egg laying food

Agar	6 g
Sucrose	6.6 g
Fruit juice	66 ml
H_2O	to 200ml

Appendix C: Plasmids

pDrive cloning vector (Qiagen)

The pDrive Cloning Vector allows UA-based ligation and easy analysis of cloned PCR products through blue/white colony screening.

pcDNA3.1/Zeo(+) (Invitrogen)

pcDNA3.1/Zeo (+) is an expression vector, derived from pcDNA3.1, designed for high-level stable and transient expression in a variety of mammalian cell lines. To this aim, it contains Cytomegalovirus (CMV) enhancer-promoter for high-level expression; large multiple cloning site; Bovine Growth Hormone (BGH) polyadenylation signal; transcription termination sequence for enhanced mRNA stability.

pUAST vector

pUAST is a P-element based vector for transgenesis in *Drosophila*. It contains five tandemly arrayed optimized GAL4 binding sites followed by the hsp70 TATA box and transcriptional start, a polylinker containing unique restriction sites and the SV40 small T intron and polyadenylation site. It also contains the *white* gene that allows the screening for successful incorporation of the transgene into the *Drosophila* genome. These features are included between the P-element ends (P3' and P5').

3. RESULTS

3.1 Datlastin localizes to the ER

Drosophila and human atlastins display remarkable homology and conservation of domain organization, likely resulting in analogous membrane topology. Inspection of the sequence of Datlastin reveals that its C-terminal aminoacid sequence KVKRS fits the di-lysine signal consensus sequence shown to be responsible for targeting transmembrane proteins to the ER either by retrieval from the Golgi apparatus or by retention (Andersson *et al.*, 1999). A di-lysine motif is also present in human atlastin-1 (Fig. 9) which, however, has been reported to distribute to Golgi (Zhu *et al.*, 2003) as well as ER membranes (Namekawa *et al.* 2007). To determine the endogenous Datlastin protein expression pattern and define precisely its subcellular localization we used three independent approaches: we used an antibody against Datlastin for immunolocalization studies, generated transgenic *Drosophila* expressing Datlastin fused with EGFP, and localized Datlastin in *Drosophila* S2 cells by immunogold transmission electron microscopy.

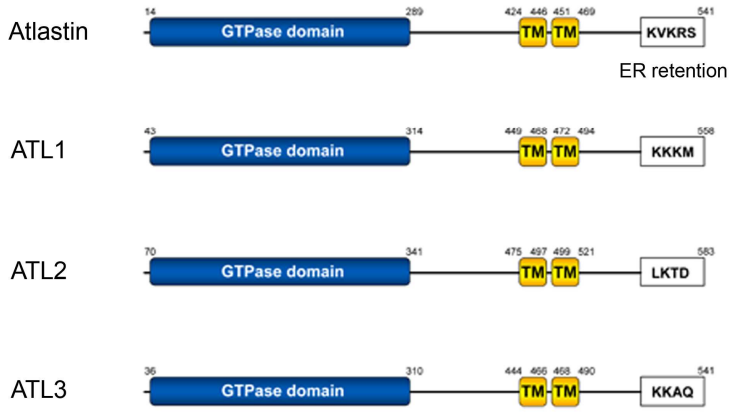

Figure 9. Schematic comparison between *Drosophila* and human atlastins. All atlastins share elevated sequence homology with precise conservation of domain organization. TM, transmembrane domain.

We performed immunohistochemistry experiments using an antibody raised against the C-terminal region of the Datlastin protein. In all the tissues and developmental stages analyzed, Datlastin was ubiquitously expressed and its expression levels appeared to be especially elevated during embryonic development. In syncitial blastoderm embryos, Datlastin immunoreactivity displayed a cytosolic distribution that consistently overlapped with the ER-specific reporter GFP-KDEL and the ER localized proteins BiP and Rtnl1-GFP (Wakefield *et al.*, 2006). Visualization of the Golgi apparatus with the GalT-GFP reporter demonstrated absence of Datlastin signal from this compartment (Fig. 10).

A transgenic *Drosophila* line expressing Datlastin C-terminally fused with EGFP (Datl-EGFP) was generated. Immunohistochemistry experiments performed in third instar larva body wall muscles showed that Datlastin-EGFP co-localized with the ER marker BiP, and did not share the punctate distribution typical of Golgi in *Drosophila* (Kondylis *et al.*, 2001), visualized with the Golgi-specific marker anti-p120 (Stanley *et al.*, 1997) (Fig. 11).

To confirm that endogenous Datlastin is restricted to the ER, we examined its localization by immunogold electron microscopy (EM). Gold labelling of Datlastin was performed in cultured *Drosophila* S2 cells and showed that Datlastin labeled almost exclusively ER membranes (Fig. 12a). Quantitative analysis of EM sections corroborated previous immunofluorescence results demonstrating that approximately 60% of gold particles were found on ER membranes (Fig. 12b). These experiments confirmed also that Datlastin was consistently absent from Golgi structures. Together, these results establish that Datlastin is a transmembrane protein residing specifically in the ER.

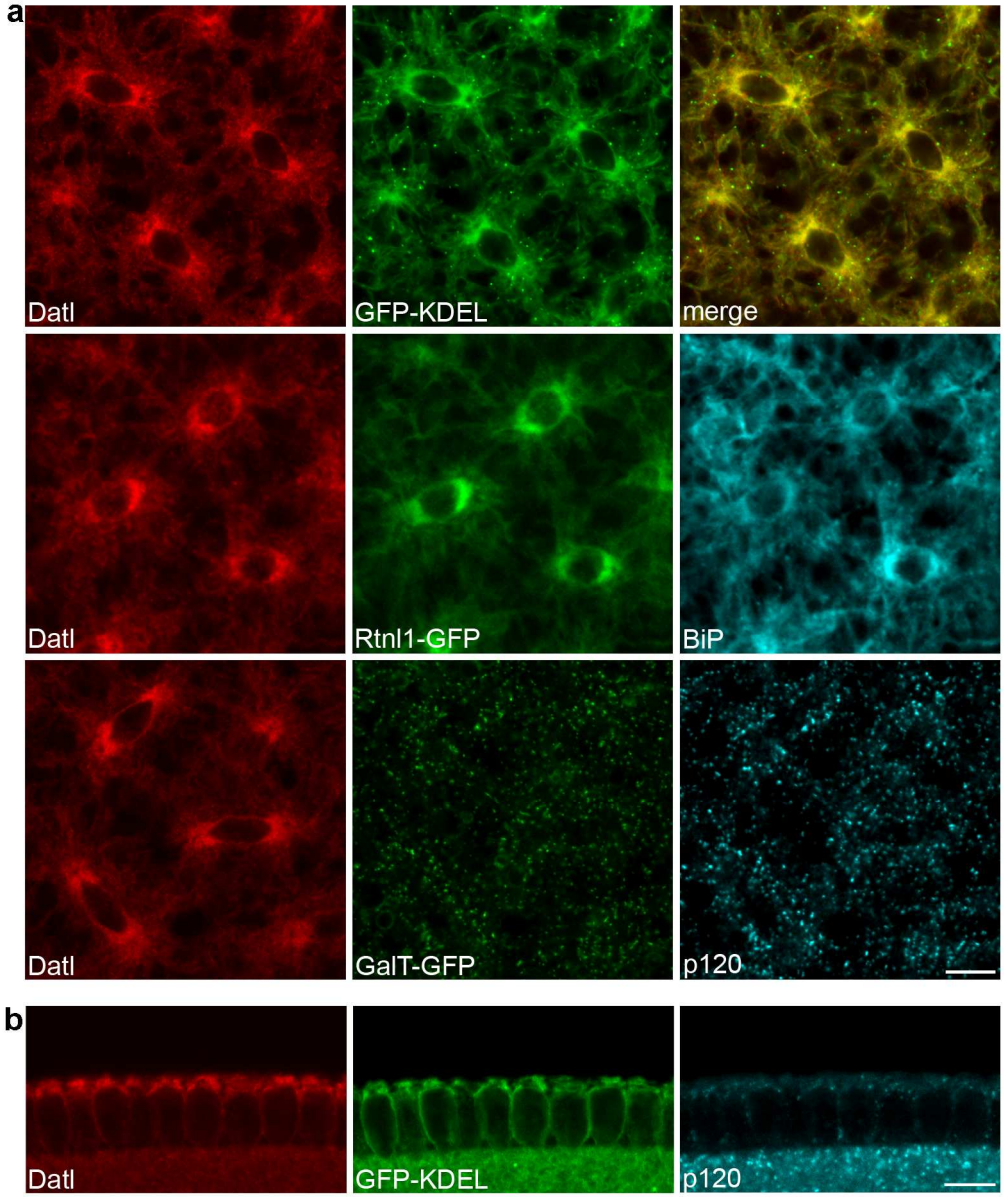

Figure 10. Endogenous Datlastin localizes on the ER. (**a**) In syncitial blastoderm embryos anti-Datlastin immunofluorescence (red) overlaps with that of the ER markers GFP-KDEL (green) (upper panels), Rtnl1-GFP (green) and BiP (cyan) (middle panels). Visualization of Golgi apparatus with the GalT-GFP reporter (green) and anti-p120 (cyan) shows that Datlastin immunoreactivity (red) does not co-localize with Golgi punctae (lower panels). Scale bar 10 μm. (**b**) Sagittal view of a cellularizing embryo labelled with anti-Datlastin antibody (red), GFP-KDEL (green) and anti-p120 antibody (cyan). Datlastin immunoreactivity overlaps with GFP-KDEL fluorescence but not with anti-p120 signal. Scale bar 10 μm.

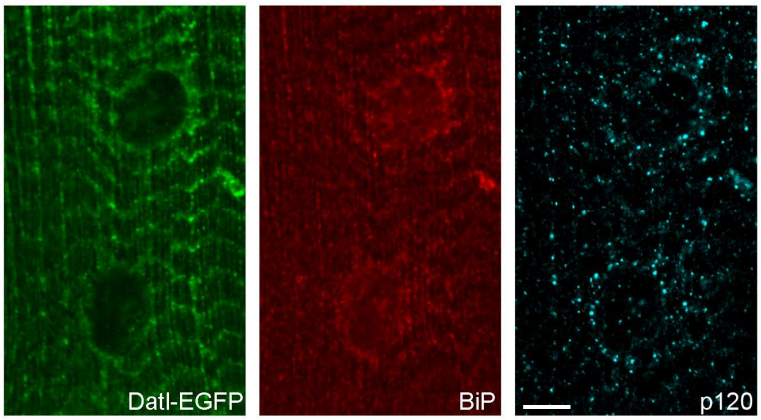

Figure 11. Datlastin-EGFP localizes on ER membranes. In third instar larva body wall muscles Datlastin-EGFP co-localizes with the ER marker BiP, but not with Golgi-specific anti-p120. Scale bar 10 µm.

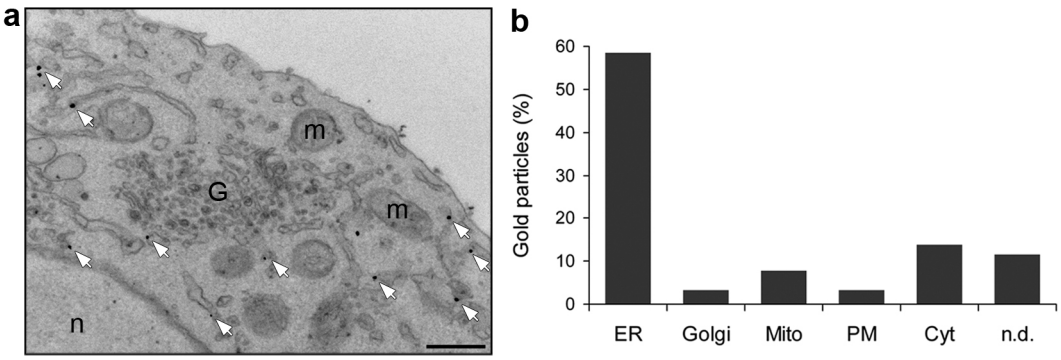

Figure 12. Endogenous Datlastin is localized on the ER in S2 cells. (a) Datlastin was localized in *Drosophila* S2 cells by immunogold labelling. Representative electron micrograph shows that gold particles localize principally on ER membranes. Scale bar 0.5 µm (m, mitochondrion; n, nucleus; G, Golgi apparatus). **(b)** The bar graph illustrates the quantitative analysis of gold particles distribution in different subcellular compartments. ER, endoplasmic reticulum; Mito, mitochondria; PM, plasma membrane; Cyt, describes gold particles that label the cytosol and do not associate with any membrane compartment; n.d. describes association with a membrane compartment not readily identifiable.

3.2 Loss of Datlastin causes ER fragmentation

To gain insight into the function of Datlastin, we examined the consequences of downregulating its expression in *Drosophila* by *in vivo* RNAi. We used UAS-Datlastin-RNAi transgenic flies, whose expression can be controlled spatially and temporally using the Gal4/UAS expression system (Brand and Perrimon, 1993). In

the UAS-Datlastin-RNAi fly line, the transgene is placed downstream of a UAS (upstream activating sequence) activation domain, that consists of GAL4-binding sites. The transgene is activated when these flies are crossed to transgenic flies that express GAL4, also known as 'drivers'. The GAL4 gene is placed downstream of a cell- or tissue-specific promoter, allowing the expression of the transgenic protein only in a specific cell or tissue type, in the progeny. A wide array of cell-type and developmentally regulated GAL4 'driver' lines have been made and characterized. Examples include the pan-neural promoter elav (embryonic lethal, abnormal vision) or the eye-specific promoter GMR (Glass Multimer Response).

Several experiments were carried out to validate the efficiency and specificity of RNAi. Ubiquitous expression of UAS-*atlastin*-RNAi using the tubulin-Gal4 driver was semi-lethal and escapers displayed small body size and shortened life span, accurately phenocopying *atl*^{1} null mutants previously described (Lee *et al.*, 2006) (Fig. 13a). We analysed lysates prepared from tubulin-Gal4/+;UAS-*atlastin*-RNAi/+ escapers by western blot. This RNAi sample showed a drastic reduction in Datlastin protein levels when compared to controls (Fig. 13b). Moreover, overexpression of UAS-*atlastin* using the eye specific driver GMR-Gal4 gave rise to a small and rough eye phenotype, which was completely suppressed by co-expression of UAS-*atlastin*-RNAi under the control of the same driver. Collectively these data demonstrate that RNAi mediated *in vivo* downregulation of Datlastin is specific and effective.

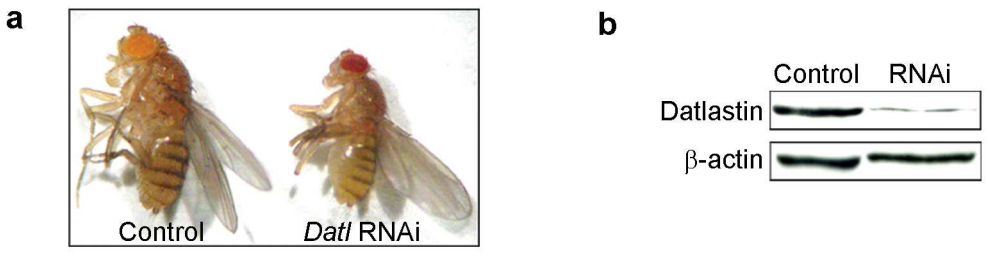

Figure 13. Efficacy of Datlastin depletion by RNAi. (a) tubulin-Gal4/+;UAS-*Datlastin*-RNAi/+ escapers phenocopy the reduced size phenotype of Datlastin null mutants; **(b)** western blot analysis of lysates prepared from tubulin-Gal4/+;UAS-*Datlastin*-RNAi/+ escapers shows that endogenous Datlastin levels are greatly decreased**.**

Because human atlastin-1 has been implicated in ER to Golgi transport, we tested the involvement of Datlastin in this process in *Drosophila*. In mammalian cells traffic impairment is known to result in disruption of Golgi morphology with dispersal of Golgi markers (Ward *et al.*, 2001). To establish whether reduced secretory traffic causes loss of Golgi staining also in *Drosophila*, we analysed the consequences of RNAi-mediated inactivation of components of the COP I and COP II coat complexes involved in ER-Golgi transport, such as α-COP and Sar-1. Immunofluorescence analysis showed that, in agreement with results in mammalian cells, RNAi-mediated inactivation of COP I and COP II coat components had dramatic consequences on Golgi morphology: the Golgi signal, visualized by GalT-GFP, was diffuse and partially redistributed to the ER (Fig. 14). We therefore monitored the morphology of this organelle in muscles and neurons of tubulin-Gal4/+;UAS-Datlastin-RNAi/+ third instar larvae. Immunofluorescence analysis of wild type control larvae using the Golgi marker p120 showed that unlike in mammalian cells, where the Golgi apparatus is exclusively localized in a perinuclear position, in all types of Drosophila cells the Golgi apparatus forms discrete punctate structures distributed throughout the cytoplasm (Kondylis et al., 2001) (Fig. 15). However, RNAi mediated downregulation of Datlastin in both neurons and muscles did not alter Golgi apparatus morphology, suggesting that transport was not affected. In contrast, examination of the ER network in knockdown tissues revealed a change in its morphology (Fig. 15). To determine normal ER morphology we used the endoplasmic reticulum marker GFP-KDEL and showed that in control neurons the ER appears as a cytoplasmic network with a few prominent punctae of staining, while in wild type body wall muscles the ER displays a punctate staining with a more filamentous distribution in proximity of the nuclei. Interestingly, downregulation of Datlastin resulted in an enrichment of punctate ER signal around nuclei, indicating that this protein may be involved in regulating ER morphology (Fig. 15).

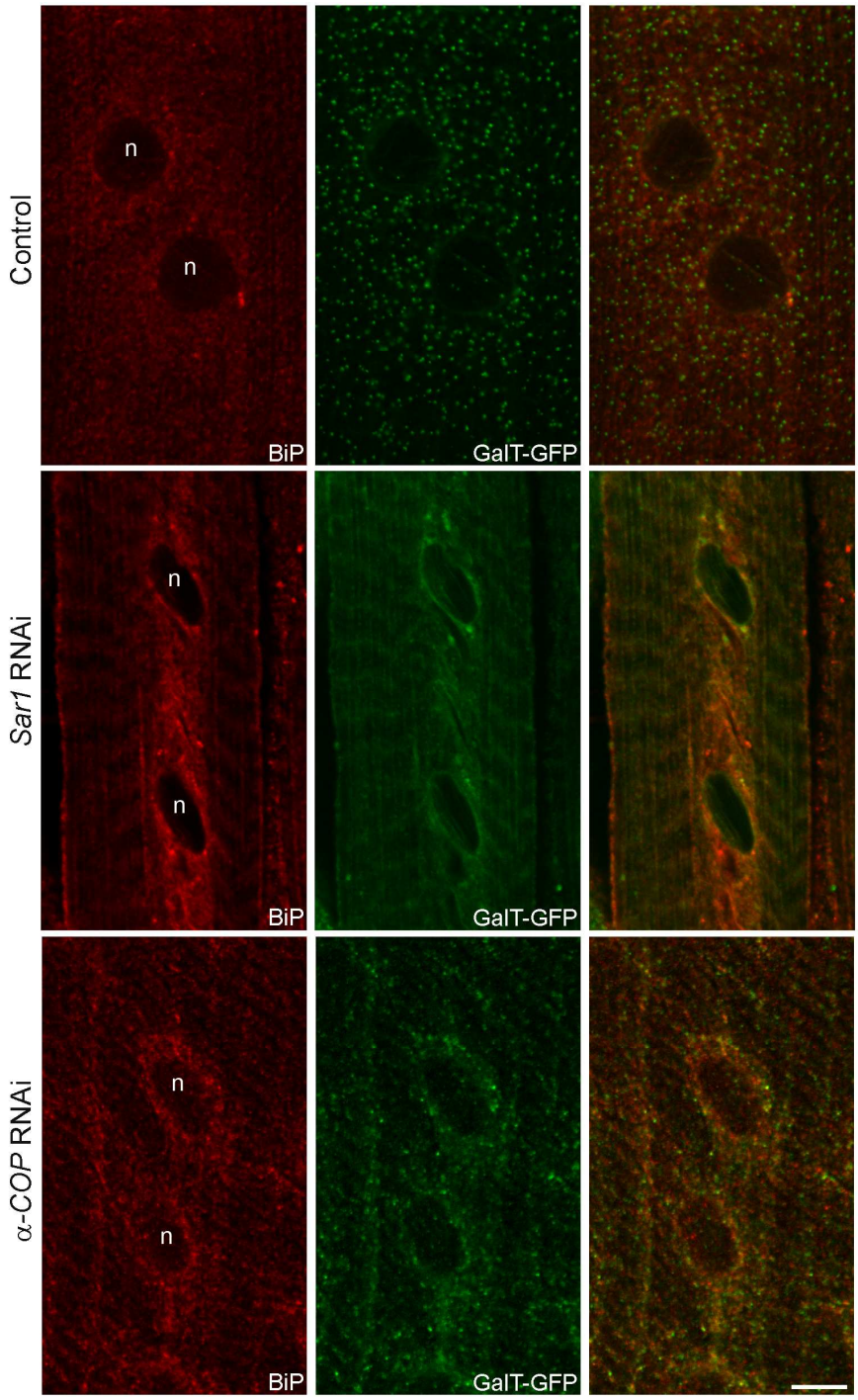

Figure 14. Disruption of COP I and COP II complexes function results in disorganization and re-distribution of the Golgi apparatus to the ER. Transgenic RNAi lines targeting α-COP and Sar1 were employed to inactivate COP I and COP II, respectively. Muscle-specific downregulation of α-COP and Sar1 driven by Mef2-GAL4 causes the normally punctuate Golgi marker GalT-GFP (green) to become diffuse and overlap with ER membranes labeled with anti-BiP antibody (red). Scale bar 10 μm.

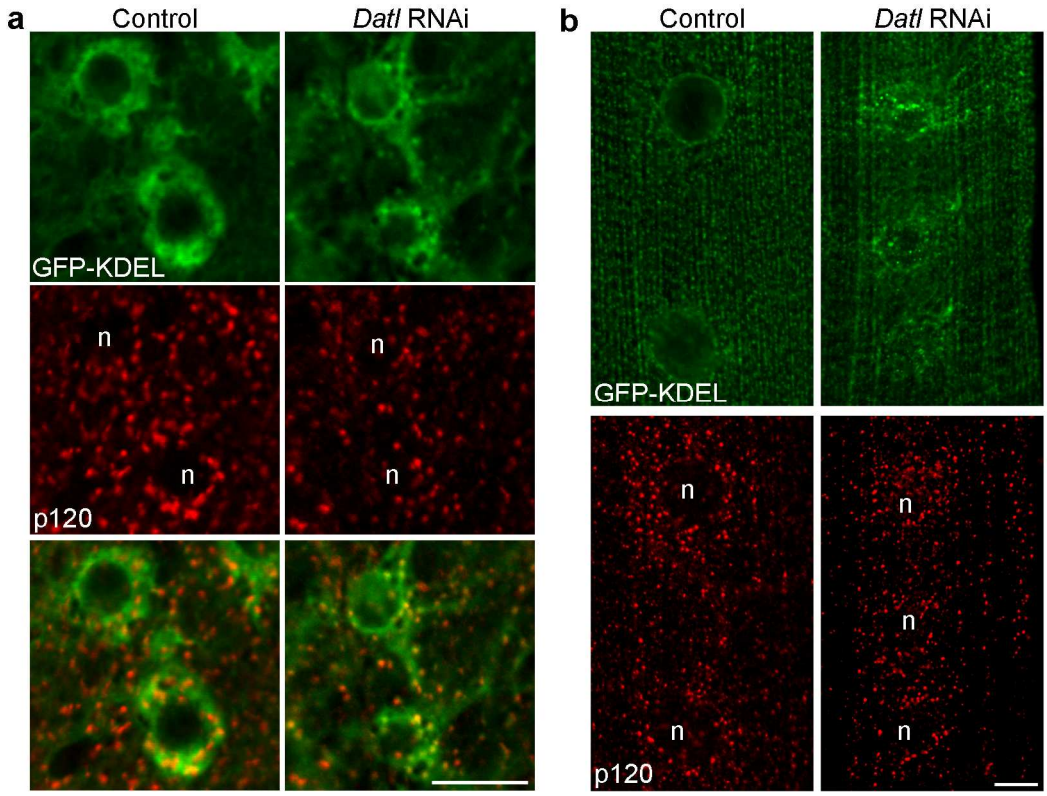

Figure 15. Immunofluorescence analysis of tissues depleted of Atlastin shows morphological defects of the ER. (a) tubulin-Gal4/UAS-GFP-KDEL;UAS-*Datlastin*-RNAi/+ larval ventral ganglion neurons and **(b)** body wall muscles were analyzed by fluorescence confocal microscopy. Loss of Datlastin in these tissues results in enrichment of ER punctae in the vicinity of nuclei as visualized using the ER reporter GFP-KDEL (green). Simultaneous labelling with the p120 marker (red) reveals that Golgi morphology is preserved. Scale bar 10 μm.

To further rule out a role for Datlastin in secretory pathway traffic, we performed two more experiments. First, we examined the morphology of ER export sites in Datlastin depleted larval muscles because maintenance of Golgi structure depends on the integrity of ER export (Ward *et al.*, 2001). To visualize ER export sites we used a protein trap line where GFP has been inserted in frame with endogenous Sar1 (Wilhelm *et al.*, 2005), a GTPase that regulates the assembly of the COP II coats at ER export sites. In tubulin-Gal4/+;UAS-*atlastin*-RNAi/+ muscles the integrity of ER export sites was preserved when compared to controls, although they became enriched near the nucleus mirroring the increased perinuclear distribution of ER punctae (Fig. 16). Second, to evaluate quantitatively the potential effects of Datlastin downregulation in trafficking through the Golgi complex, we analyzed the distribution of mCD8-GFP (Friggi-

Grelin *et al.*, 2006) in *atlastin* RNAi larva neurons. mCD8-GFP is a fusion protein between the murine lymphocyte receptor CD8 and EGFP. The receptor moves across the secretory pathway to accumulate at the plasma membrane of the cells, representing a useful reporter for intracellular transport. Transport of mCD8-GFP to the pre-synaptic membrane of the third instar larva neuromuscular junction was evaluated by quantitative analysis of GFP fluorescence intensity at the synaptic plasma membrane, and normalized to the intensity of a synaptic marker (Fig. 17a, b). Normalized GFP fluorescence intensity at wild type and *atlastin* RNAi synaptic terminals was statistically identical, demonstrating that mCD8-GFP delivery to the membrane is not impaired in *atlastin* RNAi animals (Fig. 17c).

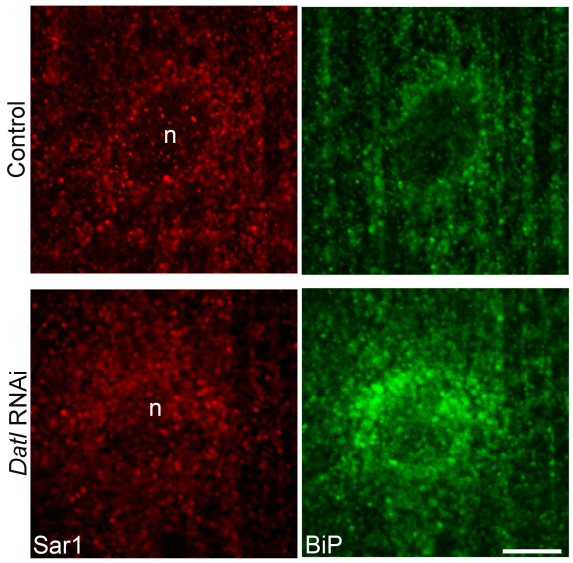

Figure 16. Endoplasmic reticulum exit sites are morphologically normal in Datlastin depleted tissue. ER exit sites marked with Sar1-GFP form small foci distributed throughout the larval muscle fibre (control) are present and essentially unchanged in tubulin-Gal4/+;UAS-*Datlastin*-RNAi/+ muscle (RNAi). In RNAi muscle, the ER visualized with anti-BiP antibody displays a characteristic perinuclear enrichment. Because of the weak fluorescence of the Sar1-GFP reporter in muscles, an anti-GFP antibody was used for better visualization. Scale bar 10 μm (n, nucleus).

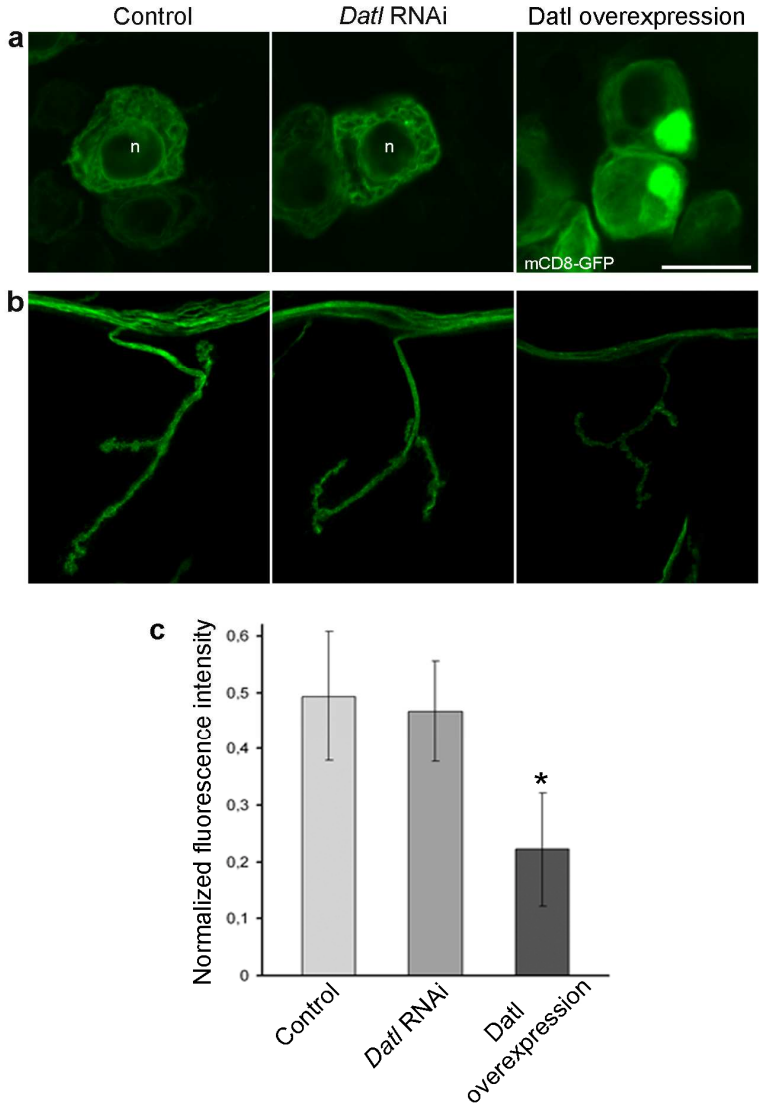

Figure 17. Datlastin overexpression, but not its downregulation, leads to transport defects. **(a)** Confocal images of individual ventral ganglion neuron bodies revealed with plasma membrane localized mCD8-GFP. mCD8-GFP distribution in controls and elav-Gal4/+;UAS-*Datlastin*-RNAi/UAS-mCD8-GFP larva brains is essentially unchanged. In motor neurons overexpressing Datlastin, mCD8-GFP fluorescence (green) displays an aberrant distribution and accumulates in globular cytoplasmic structures, absent in control neurons. **(b)** Confocal images showing the distribution of mCD8-GFP at third instar larva neuromuscular junction. mCD8-GFP fluorescence in controls and D42-Gal4/+;UAS-*atlastin*-RNAi/UAS-mCD8-GFP neuromuscular junction is essentially unchanged. In contrast, overexpression of Datlastin leads to a strong decrease of fluorescence intensity, indicating that mCD8-GFP is not properly delivered to the pre-synaptic membrane. **(c)** Histogram displaying normalized fluorescence intensity of mCD8-GFP at the third instar larva neuromuscular junction. Error bars represent s.d.. n>8; *p<0.00001. n, nucleus. Scale bars 10 μm.

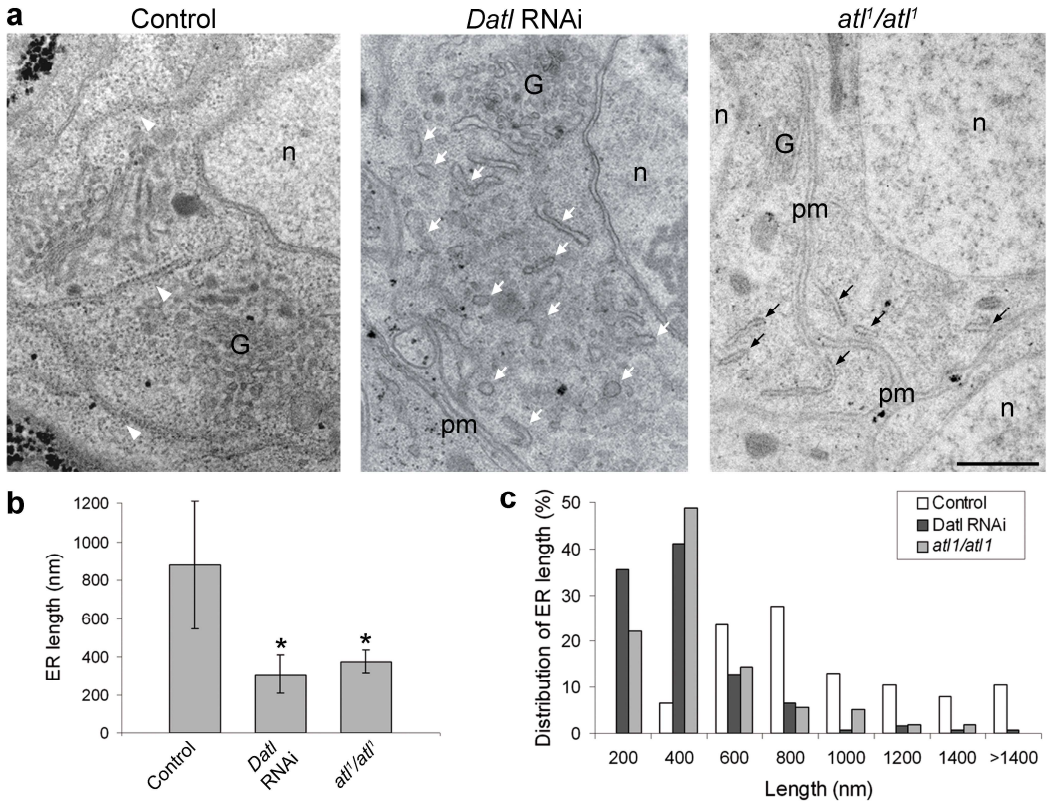

Figure 18. Loss of Datlastin causes fragmentation and discontinuity of the ER. (**a**) Electron microscopy images show that in control neurons the ER displays the typical tubular structure (arrowheads), while RNAi and *atl*^{1} neurons exhibit a fragmented ER morphology (arrows). Scale bar 0.5 μm. G, Golgi; pm, plasma membrane; n, nucleus. (**b**) Average length of ER profiles. Error bars represent s.d.; n>100; * p<0.000001. (**c**) Difference in size distribution of ER profiles.

To define in more detail the morphological alterations of the ER observed by immunofluorescence we performed transmission electron microscopy on Datlastin RNAi tissues. Ultrastructural analysis of ER morphology revealed significant alterations in both muscle fibers and neurons of Datlastin depleted larvae (Fig. 18a). Control neurons displayed long tubular ER profiles (average length 876 nm), whereas neurons lacking Datlastin showed severely undersized ER profiles (average length 308 nm) (Fig. 18b). Additionally, ER profile size distribution in Datlastin RNAi neurons revealed two classes of short ER profiles (0-200 and 200-400 nm) that were virtually absent from the cytoplasm of wild type neurons (Fig. 18c). EM analysis showed analogous shortened ER profiles in *atl*^{1} null mutant neurons, and in tubulin-Gal4/+;UAS-Datlastin-RNAi/+ muscles (Fig. 18 a-c). To demonstrate that the ER fragmentation observed was really due

to loss of Datlastin, we performed rescue experiments by expressing wild type Datlastin in the *atl*^{1} null mutant background. The presence of Datlastin fully rescued the phenotype, indicating that loss of Datlastin specifically causes ER fragmentation (Fig. 19).

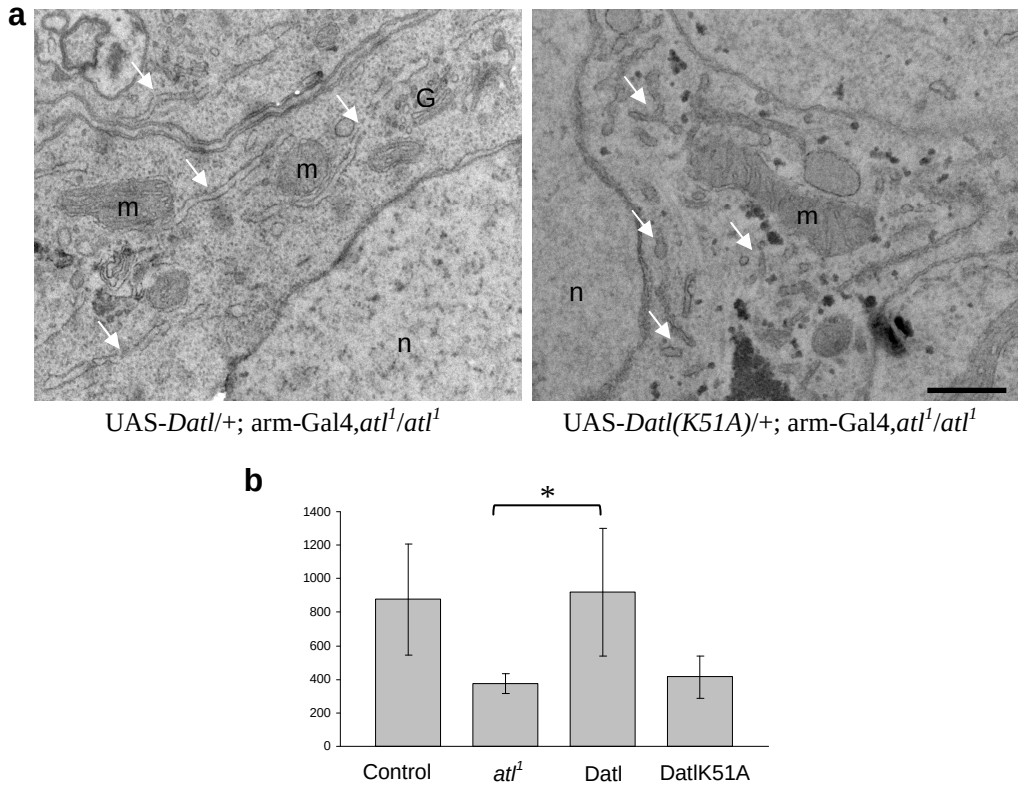

Figure 19. Expression of wild type but not K51A Datlastin rescues ER fragmentation in the *atl*^{1} null background. Wild type and mutant Datlastin were expressed at 22°C using the ubiquitous driver armadillo-Gal4. **(a)** representative EM images of third instar larva brains. n, nucleus; m, mitochondria; G, Golgi apparatus; white arrows indicate ER. Scale bar 0.5 μm. **(b)** Average ER profile length. Error bars represent s.d. n>100; * p<0,000001.

The functional consequences of these morphological changes in ER structure were examined by fluorescence loss in photobleaching (FLIP). To assess whether fragmentation in Datlastin RNAi tissues resulted in discontinuity of normally interconnected ER membranes, we targeted a GFP to ER lumen using the fusion construct UAS-GFP-KDEL and repeatedly photobleached on region of a muscle in dissected larvae. It is known that loss of a fluorescent marker from a region of a cell upon repeated photobleaching of a different region indicates continuity between the two regions. Unlike in control muscle where loss of GFP-KDEL fluorescence was homogeneous in all regions analyzed, repetitive photobleaching of GFP-KDEL in tubulin-Gal4/+;UAS-*Datlastin*-RNAi/+ muscle produced regions of unbleached fluorescence (Fig. 20), indicating that in these areas the ER network lacked its typical continuity. Fluorescence loss was still detectable in other areas suggesting that fragmentation was partial. These data reinforce our EM observations demonstrating that removal of Datlastin results in ER fragmentation. The findings that loss of Datlastin induced ER network fragmentation with loss of continuity but had no effects on Golgi architecture, did not perturb ER exit sites and did not alter mCD8-GFP membrane transport indicate that Datlastin is unlikely to participate in secretory traffic. Rather, these data strongly suggest that Datlastin function is required to maintain ER integrity.

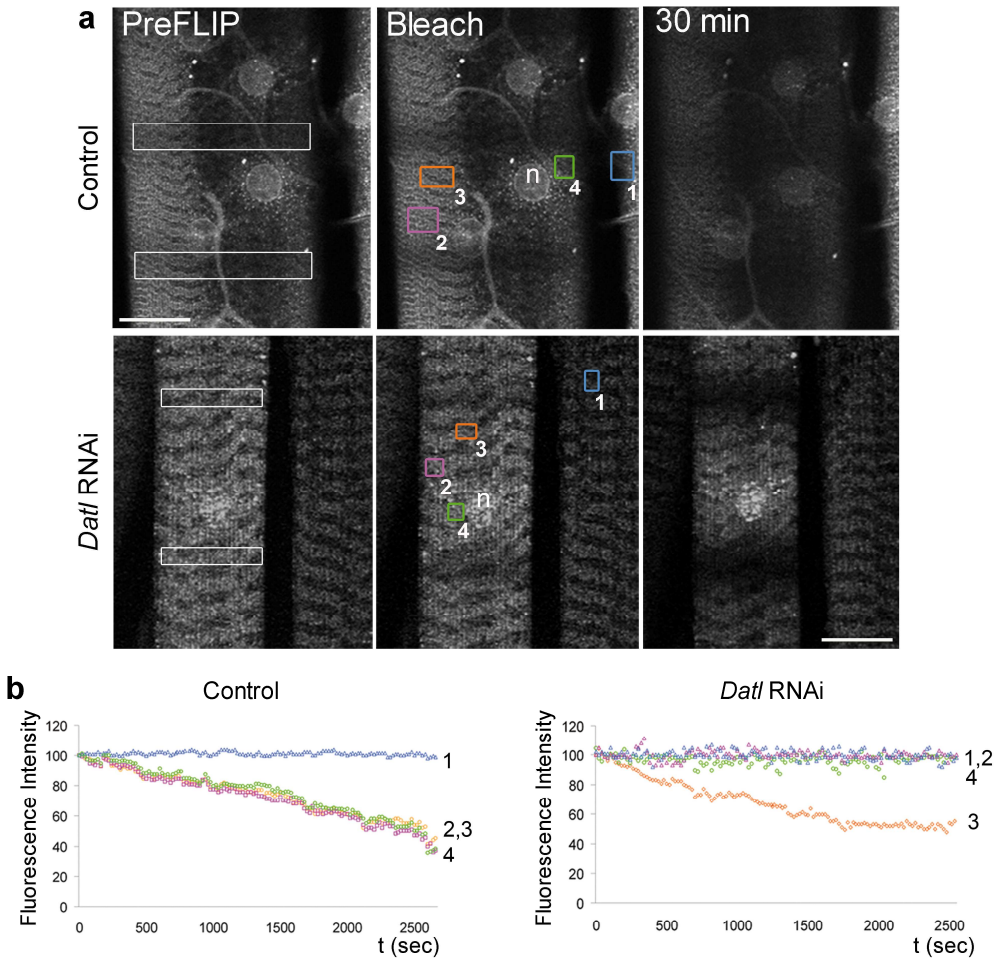

Figure 20. FLIP analysis in muscles depleted of D-atlastin demonstrates discontinuity of ER membranes. (a) Repetitive photobleaching of two ROI (white outline box) in control and Datlastin RNAi muscle expressing GFP-KDEL was performed. The bleach image represents the first image after the first photobleach. Both ROI were photobleached every 15 seconds. Fluorescence loss was analyzed in four independent regions of the muscle (colour outline box). ROI 1 was chosen on an adjacent unbleached muscle as a control. n, nucleus. Scale bar 20 µm. **(b)** Rates of loss of fluorescence for individual ROI were plotted. In control muscle all ROI lose fluorescence at a similar exponential rate. In contrast, RNAi-mediated depletion of Datlastin prevents loss of GFP-KDEL fluorescence in ROI 2 and 4, indicating discontinuity of ER structures. Fluorescence intensity of adjacent unbleached muscles (ROI 1) in both control and RNAi samples was unaffected.

3.3 Overexpression of Datlastin results in expanded ER membranes

Since reduction in Datlastin levels produced ER fragmentation, we predicted that overexpression of Datlastin may lead to excessive membrane fusion if Datlastin were involved in this process. To test this hypothesis, we used transgenic *Drosophila* for the overexpression of a myc-tagged Datlastin cDNA (UAS-*Datlastin*-myc). Gal4-mediated overexpression of UAS-*Datlastin*-myc with a number of ubiquitous and tissue specific promoters leads to lethality during early development. However, the motor neuron driver D42-Gal4 permits individuals expressing Datlastin-myc to reach pupa stages. Immunofluorescence analysis of larva brains overexpressing Datlastin-myc with the motoneuron driver D42-Gal4 showed that the ER marker BiP accumulated in cytoplasmic structures that were absent in controls (Fig. 21a). These structures were positive for myc staining as well as the Golgi marker p120, indicating that they also include Datlastin and that the Golgi apparatus is redistributed to the ER, an indication of secretory system transport blockade (Ward *et al.*, 2001).

We tested whether Datlastin overexpression might compromise endocellular traffic by monitoring ER to-plasma membrane transport of mCD8-GFP. Tissue specific overexpression of Datlastin produced an accumulation of mCD8-GFP in cytoplasmic agglomerates (Fig. 17a) positive for the ER marker BiP, indicating that mCD8-GFP was not properly delivered to the plasma membrane but was instead trapped within structures with ER identity. Moreover, quantification of mCD8-GFP fluorescence at the neuromuscular junction synapse membrane showed that transport of mCD8-GFP to the membrane was largely diminished in motor neurons overexpressing Datlastin, indicating a severe impairment of secretory traffic (Fig. 17b, c). This result indicates that upon overexpression Datlastin localizes properly but alters ER morphology and disrupts the Golgi apparatus, ultimately leading to severe transport defects.

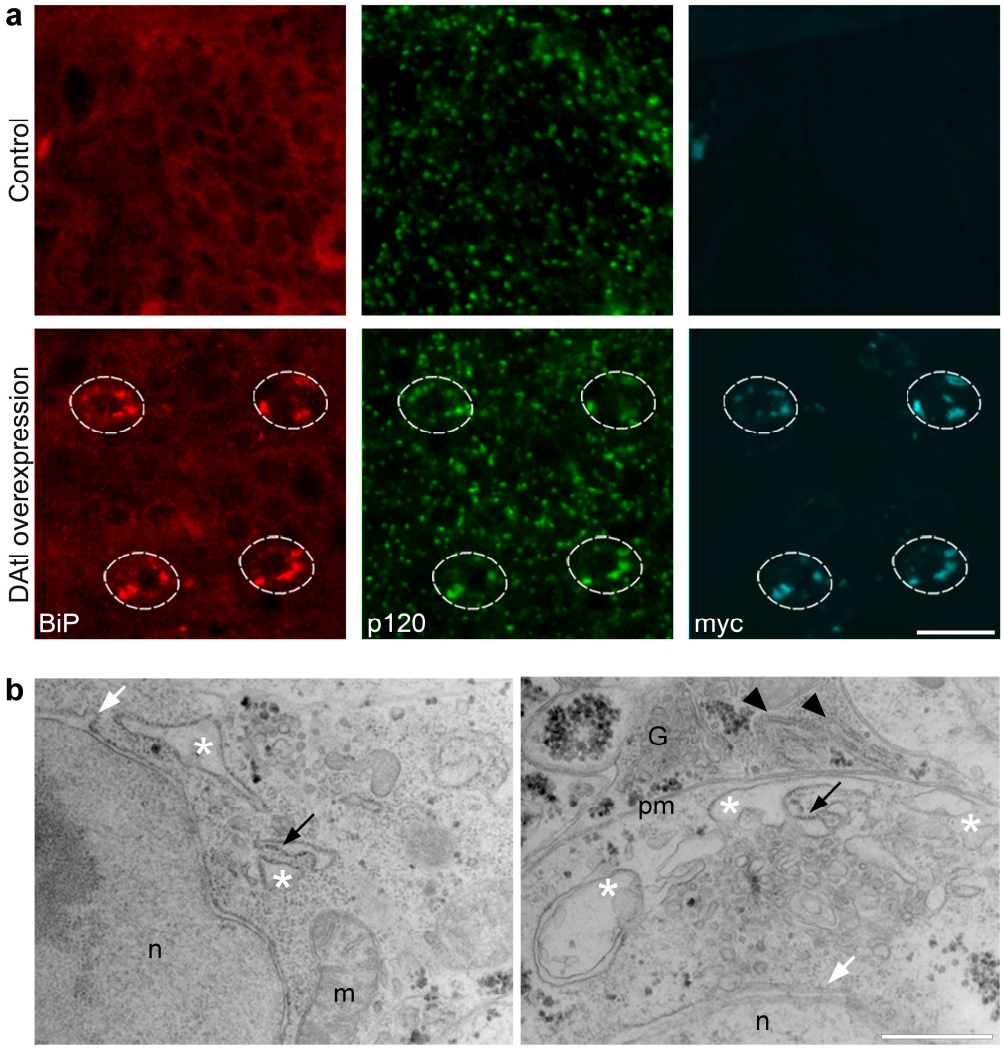

Figure 21. Datlastin induces hyper-fusion of ER membranes, homo-oligomerization and membrane tethering. (a) Overexpression of Datlastin-myc in motor neurons (white outline) induces the formation of cytoplasmic bodies with ER and Golgi identity as shown by labelling with anti-myc, anti-BiP and anti-p120 antibodies. Scale bars 10 µm. **(b)** EM analysis shows that neurons overexpressing Datlastin exhibit ER (asterisks) and nuclear envelope (white arrows) expansion. Note a non-overexpressing neuron with normal tubular ER morphology (black arrowheads). Scale bar 0.5 µm. G, Golgi; m, mitochondrion; n, nucleus; pm, plasma membrane; ribosomes, black arrows.

Ultrastructural analysis of D42-Gal4/+;UAS-*Datlastin*-myc/+ motor neurons by transmission electron microscopy confirmed that Datlastin overexpression disrupts the ER network. Normally tubular ER profiles were absent in Datlastin overexpressing motoneurons where ER membranes formed expanded cisternae (Fig. 21b). This expansion of ER elements is consistent with an increase in membrane fusion and suggests that Datlastin itself could directly

mediate bilayer merger. In agreement with immunofluorescence data, normal Golgi complexes were essentially absent in neurons overexpressing Datlastin (Fig. 21b). Absence of normal Golgi, redistribution of Golgi proteins to the ER and impaired transport of mCD8-GFP to the plasma membrane suggest a block in secretory traffic indicating that excessive fusion of ER membranes brought about by Datlastin severely impairs secretory traffic.

3.4 Datlastin mediates tethering of ER membranes

Previous studies have shown that all three human atlastins can self-assemble into oligomeric complexes (Zhu *et al.*, 2003; Rismanchi *et al.*, 2008). We therefore performed co-immunoprecipitation studies to establish whether Datlastin was also capable of homo-oligomerization. HeLa cells were simultaneously transfected with Datlastin-myc and Datlastin-HA constructs and immunoprecipitated using anti-myc antibodies. Datlastin-HA was found in the pellet, demonstrating that Datlastin molecules are able to self-associate (Fig. 22a).

This finding, together with the observations that atlastins are transmembrane proteins, that Datlastin localizes to ER membranes, that its downregulation triggers ER fragmentation and its overexpression causes expansion of ER elements, raised the possibility that Datlastin could be directly involved in tethering adjacent ER membranes thereby permitting homotypic fusion to occur. To test this hypothesis, membrane vesicles were prepared from HeLa cells transfected with Datlastin. Transfected cells were homogenized in the absence of detergent and fragmented membranes were vesiculated by sonication. Fractionation of cleared cell homogenates showed that Datlastin and the ER resident integral membrane protein calnexin partitioned exclusively to the membrane fraction while the ER-lumenal protein PDI remained in the soluble fraction (Fig. 22c). This demonstrates that under these lysis conditions Datlastin remained properly associated with membranes, permitting us to probe by co-immunoprecipitation whether Datlastin self-association occurred between distinct vesicles. Membrane vesicles were prepared from HeLa cells separately transfected with Datlastin-myc or Datlastin-HA, then mixed and immunoprecipitated. When

anti-myc antibodies were used to precipitate Datlastin-myc harbouring vesicles, Datlastin-HA was recovered in the pellet, demonstrating that Datlastin molecules inserted in adjacent ER membranes can form trans complexes (Fig. 22b). These results establish that homophilic interactions between Datlastin molecules provide a tethering step between opposing ER membranes leading to bilayer merger potentially mediated directly by Datlastin.

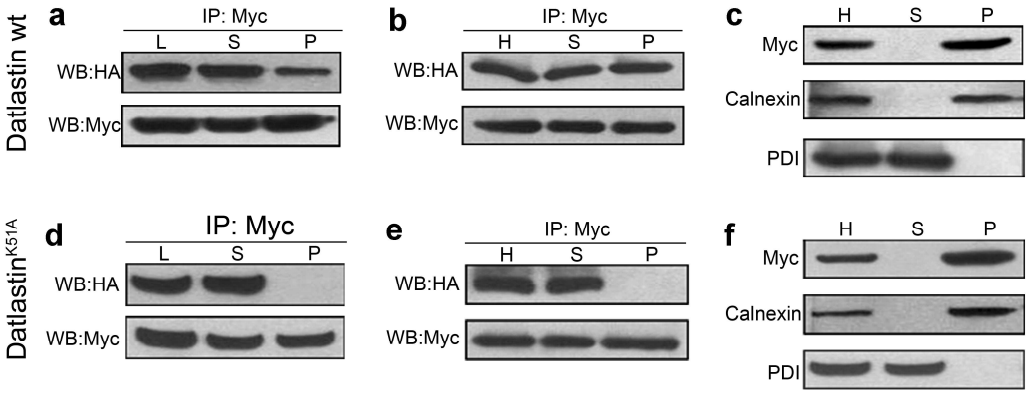

Figure 22. Wild type but not K51A Datlastin self-associates and mediates membrane tethering. (a) Lysates from HeLa cells co-transfected with wild type Datlastin-myc and Datlastin-HA were immunoprecipitated and analyzed by western blot. **(b)** Membrane vesicles from HeLa cells expressing Datlastin-HA or Datlastin-myc were mixed, immunoprecipitated and analyzed by western blotting. **(c)** Western blot analysis of the soluble and membrane fractions from cell homogenates. **(d)** Anti-Myc immunoprecipitates from HeLa cells co-transfected with Datlastin^{K51A}-HA and Datlastin^{K51A}-myc are devoid of Datlastin^{K51A}-HA. **(e)** A vesicle immunoprecipitation assay demonstrates the inability of Datlastin^{K51A} to mediate tethering. **(f)** Western blot analysis of the soluble and membrane fractions from Datlastin^{K51A}-expressing cell homogenates. L, lysate; H, cell homogenate; S, supernatant; P, pellet.

3.5 Datlastin drives membrane fusion *in vitro*

A direct role for Datlastin in membrane fusion was tested *in vitro* in a liposome fusion assay performed in collaboration with the laboratory of James McNew at Rice University (Houston). This is a lipid-mixing assay based on fluorescence resonance energy transfer (FRET) between two fluorophores linked to phospholipids. One set of liposomes (donor liposomes) contains phospholipids whose head groups are labeled with the FRET pair rhodamine and NBD. The rhodamine and NBD are at a concentration where most of the NBD signal is

quenched by rhodamine. If donor liposomes are mixed with a set of unlabeled liposomes (acceptor liposomes) and fusion occurs, the NBD and rhodamine concentration would halve, the distance between the fluorophores increase and there would be an increase in NBD signal that can be measured over time. Normally there is minimal fusion between individual liposomes and thus NBD signal does not increase significantly over time. When recombinant GST-Datlastin was reconstituted into donor and acceptor liposomes and magnesium and GTP were added, a robust increase in NBD fluorescence was seen over time, indicating that Datlastin can mediate membrane fusion *in vitro* (Fig. 23a).

No fluorescence increase was seen in the absence of GTP, suggesting that fusion is completely dependent on GTPase activity. Moreover, no fusion was seen with GDP, GMP, ATP or when magnesium is replaced with calcium. Additionally, dynamic light scattering experiments and analysis of negative stained Datlastin proteoliposomes by EM showed an increase in size of the proteoliposome population after fusion (Fig. 24). These data demonstrate that Datlastin alone is sufficient to drive membrane fusion *in vitro*.

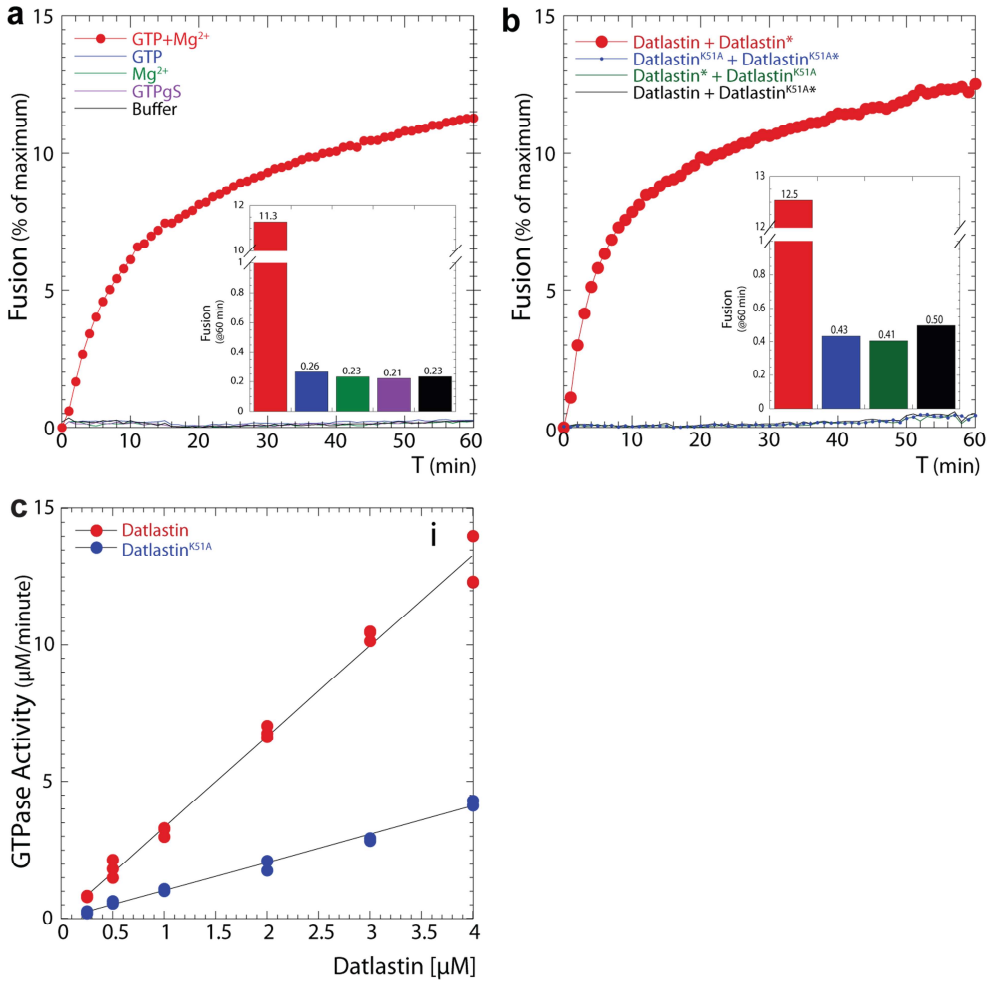

Figure 23. Datlastin mediates proteoliposome fusion. (a) Kinetic fusion graph of unlabeled Datlastin acceptor proteoliposomes fused with equimolar fluorescently labeled Datlastin donor proteoliposomes. NBD fluorescence was measured at one minute intervals and detergent was added at 60 minutes to determine maximum fluorescence. Inset histogram: extent of fusion at 60 minutes. **(b)** Fusion reactions were performed with either donor and/or acceptor proteoliposomes containing Datlastin^{K51A}. Donor liposomes are indicated with an asterisk. Inset histogram: extent of fusion at 60 minutes. **(c)** GTPase activity of increasing concentrations of wild type and K51A Datlastin.

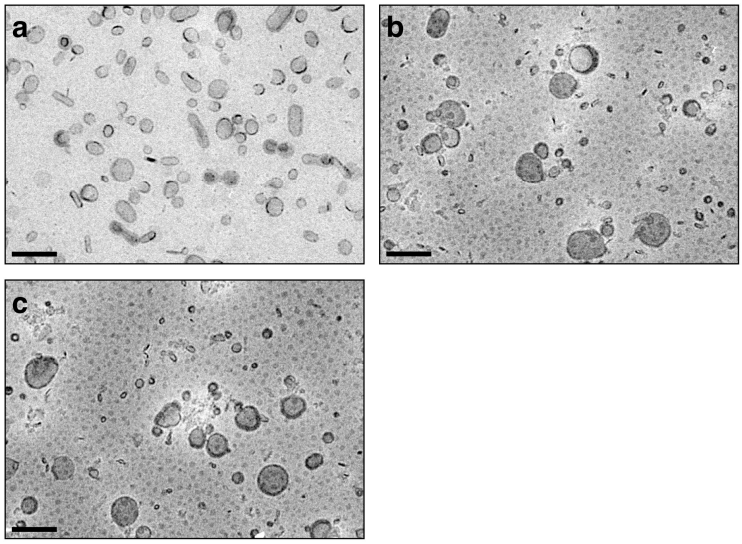

Figure 24. Transmission electron microscopy of negative stained Datlastin proteoliposomes. (a) Unfused Datlastin proteoliposomes incubated without GTP. **(b** and **c)** Fused Datlastin proteoliposomes incubated with 2 mM GTP and 5 mM Mg^{2+} for 15 min at 37°C. Scale bars 200nm.

3.6 Datlastin function requires GTPase activity

We postulated that Datlastin mediated tethering and fusion of ER membranes should rely on the GTPase activity of Datlastin. To test this hypothesis, we generated transgenic flies for the expression of Datlastin carrying a K51A substitution (UAS-Datlastin^{K51A}-myc) in the P-loop of the GTP-binding domain, and verified that protein expression levels were comparable to those of UAS-*Datlastin*-myc transgenics. Replacement of the corresponding lysine in other GTP-binding proteins is known to significantly lower or abolish nucleotide binding affinity thus preventing GTP hydrolysis and protein function (Praefcke *et al.*, 2004). Biochemical analysis of recombinant wild type and K51A mutant Datlastin indicates that replacement of lysine 51 significantly reduces GTPase activity (Fig. 23c). Consistent with this notion, GMR-Gal4 driven eye specific expression of UAS-Datlastin^{K51A}-myc had no phenotypic effects, while expression of UAS-Datlastin-myc gave rise to a small and rough eye phenotype (Fig. 25a-c). Moreover, in contrast to overexpression of wild type Datlastin, overexpression of

Datlastin^{K51A} with all drivers allowed survival of the flies, implying that replacement of lysine 51 with alanine results in the inactivation of the protein.

Importantly, immunofluorescence analyses of motor neurons expressing Datlastin^{K51A}-myc under the control of D42-Gal4 showed that Datlastin^{K51A} properly localized to the ER and the tissues were devoid of the globular tangles of ER membranes seen upon overexpression of wild type Datlastin (Fig. 25d), indicating that ER and Golgi were unaltered. Unlike the wild type protein, when expressed in the *atl*^{1} null mutant background, Datlastin^{K51A} was unable to rescue ER fragmentation in *atl*^{1} neurons (Fig. 19). These observations demonstrate that formation of aberrant ER depends crucially on the GTPase activity of Datlastin.

To understand how loss of GTPase activity might impair Datlastin function, we examined the ability of the GTPase deficient Datlastin^{K51A}-HA and Datlastin^{K51A}-myc to homo-oligomerize in co-transfected HeLa cells as well as in the membrane vesicle co-immunoprecipitation assay. In both assays, Datlastin^{K51A} was unable to self-associate (Fig. 22d-f) indicating that this inability prevented the formation of trans-oligomeric complexes between Datlastin^{K51A}-HA and Datlastin^{K51A}-myc harbouring vesicles. Thus GTPase activity is critical for self-association and GTPase-deficient Datlastin^{K51A} lacks the competence to mediate membrane tethering.

Given that Datlastin^{K51A} was unable to oligomerize, we tested its ability to drive fusion. Donor and acceptor proteoliposomes containing equal amounts of Datlastin^{K51A} or wild type Datlastin were prepared and their ability to fuse analyzed. When wild type Datlastin was incorporated in both membranes, fusion proceeded normally; however, inclusion of Datlastin^{K51A} in the reaction failed to support fusion (Fig. 23b). This result demonstrates that a functional GTPase domain is required on both membranes for fusion to occur.

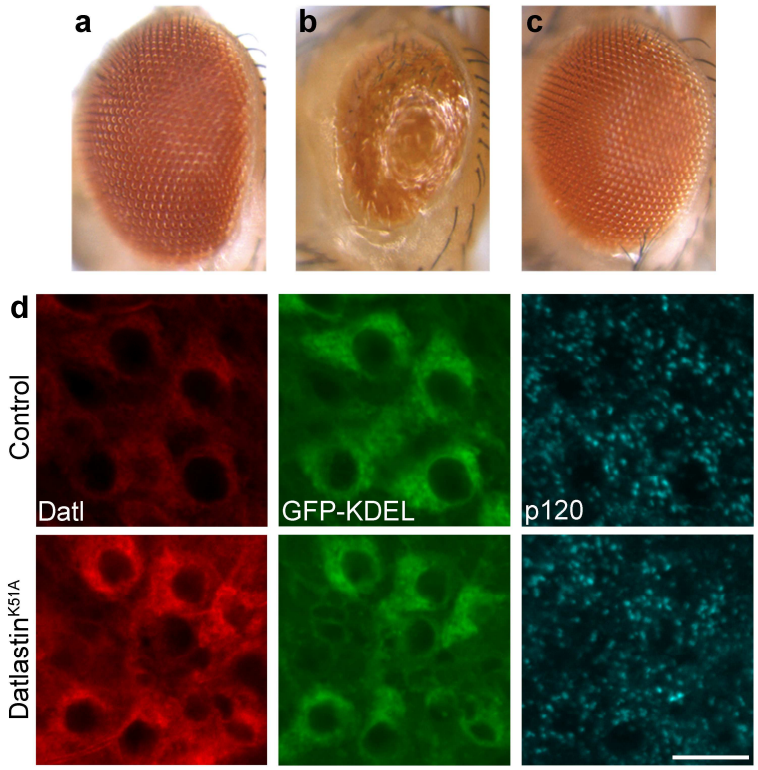

Figure 25. GTP-ase deficient Datlastin is inactivate and unable to mediate membrane tethering and fusion. (a) Adult *Drosophila* eye. **(b)** Overexpression of Datlastin using GMR-Gal4 generates a small eye. **(c)** Eye overexpression of Datlastin^{K51A} has no phenotypic consequences. **(d)** Simultaneous visualization of GFP-KDEL (green), Golgi p120 (blu) and Datlastin^{K51A} (red) of tubulin-Gal4/+;UAS-*Datlastin*^{K51A}-myc /+ ventral ganglion neurons.

4. DISCUSSION

Establishment of the ER network occurs via a basic homotypic fusion reaction that requires GTP hydrolysis and membrane-associated factors (Dreier and Rapoport, 2000; Voeltz *et al.*, 2006) suggesting the involvement in this process of a GTPase located on the ER membrane. Formation of a tubular network then ensues that relies on the action of cytosolic protein components (Voeltz *et al.*, 2002). While reticulons are the major players in tubularization of the ER (Voeltz *et al.*, 2006), no obvious candidates responsible for mediating homotypic fusion of ER membranes have been identified.

Our combined *in vivo* and *in vitro* analyses provide strong evidence that Datlastin is the key GTPase required for homotypic fusion of ER membranes. Datlastin, a GTPase belonging to the dynamin superfamily of GTPases, specifically localizes in the ER, a localization consistent with a role in mediating homotypic interactions between ER membranes. In response to loss of Datlastin the ER network becomes fragmented, supporting a function in maintenance of ER integrity. Datlastin is capable of homo-oligomerization and self-association can occur within the same membrane as well as between opposing membranes. This property leads to the formation of trans complexes that tether adjacent ER membranes. *In vivo* overexpression of Datlastin results in the expansion of ER elements, consistent with excessive membrane fusion. In agreement with our interpretation of *in vivo* overexpression results, recombinant Datlastin potently drives membrane fusion *in vitro* in a GTP dependent manner. Datlastin requires GTPase activity to exert its function because GTPase-deficient Datlastin^{K51A} is functionally inactive *in vivo*, fails to tether ER membranes due to inability to homo-oligomerize, and does not promote membrane fusion *in vitro*. It is likely that the inability of Datlastin^{K51A} to fuse is directly related to its inability to self-associate.

No obvious transport impairment was observed in response to loss of Datlastin, demonstrating that the protein is not involved in the secretory pathway. Nevertheless, subtle transport defects due to architectural disorganization of the

ER following fragmentation cannot be ruled out completely. Reduced membrane traffic in *Drosophila* results in cell growth defects (Lee and Cooley, 2007), indicating that minor transport impairment secondary to ER disorganization may explain the small size of *Datlastin* mutant cells and individuals.

If Datlastin is crucial to promote membrane fusion and thus plays a fundamental role in ER biogenesis, it would be reasonable to expect that loss of protein function would result in embryonic lethality. However, both *atlastin* null mutant and knockdown flies partially make it to adulthood. Immunohistochemistry experiments showed that Datlastin expression levels are elevated during embryonic development especially in syncytial and cellularizing blastoderm when the embryo develops under the control of maternally provided proteins (Lee *et al.*, 2006). It is therefore likely that the robust maternal contribution, possibly coupled to slow protein turnover, allows progression through development. *Drosophila* eggs inherit a vast deposit of maternal gene products, which can mask the effect of zygotic loss of gene products until late in embryogenesis or well into larval development depending of the longevity of the gene product. The observation that surviving *Datlastin* mutant females are sterile due to an inability to produce mature eggs (Lee *et al.*, 2006), further underscores the importance of Datlastin in development. Deposition of maternal Datlastin would therefore ensure that ER biogenesis occurs unscathed throughout development. ER fragmentation set off by *atlastin* RNAi-mediated downregulation becomes manifest during larva development probably arising when maternally provided Datlastin becomes limiting and zygotic transcripts are eliminated by RNAi. Therefore, the observed fragmentation likely reflects a deterioration of ER maintenance rather than loss of *de novo* ER biogenesis.

The identification of Datlastin as the central component of the ER machinery devoted to homotypic fusion raises important questions concerning the mechanistic details of Datlastin mediated tethering and fusion of membranes. Datlastin is a transmembrane protein with membrane topology resulting in the N- and C-termini being exposed to the cytoplasm and available for homo-oligomerization and promotes fusion in a GTPase-dependent manner. We propose that upon nucleotide binding, Datlastin molecules inserted within adjacent ER

membranes become competent to self-association thus bringing the two ER membranes into very close apposition. The GTPase catalytic activity of dynamin superfamily members can be stimulated by oligomerization (Praefcke *et al.*, 2004). Likewise, Datlastin complex formation could stimulate GTP hydrolysis supplying the energy necessary for membrane destabilization eventually leading to fusion.

Membrane fusion in general requires molecules that tether membranes, molecules that bring them into close apposition and molecules that disturb the lipid bilayers locally to overcome the energy barriers preventing fusion. In SNARE-mediated fusion these functions are carried out by different sets of proteins. During ER homotypic fusion, Datlastin provides all these tasks representing the only non-viral protein capable of unaided fusion and, together with SNAREs, the only fusogenic protein so far identified in eukaryotes.

While mitochondria have been believed to use unique fusion mechanisms because they do not rely on either SNAREs or the AAA-ATPase NSF, our findings imply that membrane fusion brought about by dynamin-like GTPases is more widespread and is involved at least in morphogenesis and maintenance of the ER. It is tempting to speculate that while heterotypic fusion events involving membranes of different origin such as those responsible for secretory pathway trafficking, exocytosis and neurotransmitter release, depend on SNAREs and NSF based machineries, large GTPase-mediated mechanisms may underlie homotypic membrane fusion in general. This modality of fusion may have evolved because it permits to conveniently achieve specificity, thus preserving organelle identity, by entrusting the execution of homotypic fusion reactions to the interaction between molecules of the same organelle-specific protein residing on adjacent membranes.

A recent report (Hu *et al.*, 2009) indicated that human atlastins are specifically associated with reticulons and DP1, suggesting that atlastins may interact generally with this class of ER tubule-shaping proteins. This result is further supported by genetic interactions in yeast indicating a synthetic negative relationship between mutations in orthologous atlastin (SEY1) and DP1 (YOP1) genes. Moreover, a cell free assay that recapitulates formation of ER tubular

networks in frog egg extracts was strongly inhibited upon addition of neutralizing atlastin antibodies, indicating a direct role for the altlastin proteins in shaping tubular ER networks (Hu *et al.*, 2009). The collective findings seem consistent with a model in which reticulons/DP1 produce tubules and atlastin GTPases introduce branch points in the ER network through homotypic membrane fusion. It should be informative to test if membrane networks are generated in a minimal proteoliposome system reconstituted with purified reticulons, DP1, and atlastin, although it is possible that, given the varied ER morphologies that are observed in distinct cell types and at different stages of the cell cycle, additional components will be involved to assemble and maintain reticular networks.

Atlastin-1 belongs to a group of genes implicated in hereditary spastic paraplegia (HSP), a neurological disorder characterized by axonal degeneration of long corticospinal motor neurons. Over half of the HSP mutations reside in three genes that include atlastin-1, spastin and REEP1, another member of the DP1 family of proteins (Depienne *et al.*, 2007). A properly functioning ER is absolutely required for all cells given that it is the initial way station for most secreted proteins and plasma membrane proteins. Disturbance in the function or loss of integrity of the ER could result in a failure of protein folding, glycosylation, or transport leading to ER stress that ultimately may contribute to the pathogenesis of neurodegenerative disorders (Lindholm *et al.*, 2006). Long spinal neurons appears to be particularly dependent on a functioning ER networks for cell function. Independently of their mechanism, pathological mutations in atlastin-1 are likely to perturb membrane fusion with loss of ER integrity suggesting that progressive axonal degeneration in SPG3A patients may be the consequence of ER stress engendered by this perturbation.

Our studies have uncovered a requirement for Datlastin in the homotypic fusion of ER membranes, suggesting that Datlastin represents the GTPase activity postulated to be required for this process. Although further studies will be necessary to dissect the structural basis of Datlastin function, the identification of its fusogenic properties lays the foundation for understanding the mechanisms underlying ER biogenesis and maintenance and may contribute to a better understanding of neuronal degeneration in Hereditary Spastic Paraplegia.

5. REFERENCES

Allan, V.J. and Vale, R.D. (1991) Cell cycle control of microtubule-based membrane transport and tubule formation in vitro. J. Cell Biol., 113, 346–359.

Andersson, H., Kappeler, F. and Hauri, H. P. (1999) Protein targeting to endoplasmic reticulum by dilysine signals involves direct retention in addition to retrieval. *J. Biol. Chem.* **274**, 15080-4.

Antonin, W., Fasshauer, D., Becker, S., Jahn, R. and Schneider, T. R. (2002) Crystal structure of the endosomal SNARE complex reveals common structural principles of all SNAREs. *Nat. Struct. Biol.* **9**, 107 – 111.

Baumann, O. and Walz, B. (2001) Endoplasmic reticulum of animal cells and its organization into structural and functional domains. *Int. Rev. Cytol.*, **205**, 149–214.

Bier, E. (2005) *Drosophila*, the golden bug, emerges as a tool for human genetics. *Nat. Rev. Genet.* **6,** 9–23.

Brand, A. H. & Perrimon, N. (1993) Targeted gene expression as a means of altering cell fates and generating dominant phenotypes. *Development*, **118**, 401-15.

Cai, H., Reinisch, K. and Ferro-Novick, S. (2007). Coats, tethers, Rabs, and SNAREs work together to mediate the intracellular destination of a transport vesicle. Dev. Cell 12, 671 – 682.

Cauchi, R.J., van den Heuvel, M. (2006) The Fly as a Model for Neurodegenerative Diseases: Is It Worth the Jump? *Neurodegenerative Dis*, **3**, 338–356.

Celotto, A., Palladino, M. (2005) Fly models of neurodegeneration. *Molecular intervention*, **5**, 292-303.

Chernomordik, L. V. and Kozlov, M. (2008) Mechanics of membrane fusion. *Nat. struc mol boil*, **15**(7):675-83.

Collas, I. and Courvalin, J.C. (2000) Sorting nuclear membrane proteins at mitosis. *Trends Cell Biol.*, **10**, 5–8.

Dayel, M.J. and Verkman, A.S. (1999) Diffusion of green fluorescent protein in the aqueous-phase lumen of the endoplasmic reticulum. *Biophys. J.*, **76**, 2843–2851.

Depienne, C., Stevanin, G., Brice, A. and Durr, A. (2007) Hereditary spastic paraplegias: an update. *Curr Opin Neurol*, **20**, 674-80.

Dreier, L. and Rapoport, T.A. (2000) *In vitro* formation of the endoplasmic reticulum occurs independently of microtubules by a controlled fusion reaction. *J. Cell Biol.*, **148**, 883–898.

Eccleston, J.F., Binns, D.D., Davis, C.T., Albanesi, J.P., Jameson, D.M. (2002) Oligomerization and kinetic mechanism of the dynamin GTPase. *Eur. Biophys. J.*, **31** 275–282.

Ellenberg, J., Siggia, E.D., Moreira, J.E., Smith, C.L., Presley, J.F., Worman, H.J. and Lippincott-Schwartz, J. (1997) Nuclear membrane dynamics and reassembly in living cells: targeting of inner nuclear membrane protein in interphase and mitosis. *J. Cell Biol.*, **138**, 1193–1206.

Friggi-Grelin, F., Rabouille, C. & Therond, P. (2006) The cis-Golgi *Drosophila* GMAP has a role in anterograde transport and Golgi organization *in vivo*, similar to its mammalian ortholog in tissue culture cells. *Eur. J. Cell. Biol.*, **85**, 1155-66.

Gant, T.M. and Wilson, K.L. (1997) Nuclear assembly. *Annu. Rev. Cell Dev. Biol.*, **13**, 695–699.

Grosshans, B. L., Ortiz, D. and Novick, P. (2006) Rabs and their effectors: achieving specificity in membrane traffic. *Proc. Natl. Acad. Sci. USA*, **103**, 11821 – 11827.

Harrison, S. (2008) Viral membrane fusion. *Nat struct mol boil*, **15**(7):690-8.

Hetzer, M., Meyer, H.H., Walther, T.C., Bilbao-Cortes, D., Warren, G. and Mattaj, I.W. (2001) Distinct AAA-ATPase p97 complexes function in discrete steps of nuclear assembly. *Nat. Cell Biol.*, **3**, 1086–1091.

Hoppins, S. and Nunnari, J. (2009) The molecular mechanism of mitochondrial fusion. *Biochimica et Biophysica Acta*, **1793**, 20–26.

Hu, J., Shibata, Y., Zhu, P., Voss, C., Rismanchi, N., Prinz, W. A., Rapoport, T. A., and Blackstone, C. (2009) A Class of Dynamin-like GTPases Involved in the Generation of the Tubular ER Network. Cell **138**, 549–561.

Hua, Y., Scheller, R. H. (2001) Three SNARE complexes cooperate to mediate membrane fusion. *Proc. Natl. Acad. Sci. USA*, **98**, 8065.

Ishihara, N., Eura, Y., Mihara, K. (2004) Mitofusin 1 and 2 play distinct roles in mitochondrial fusion reactions via GTPase activity. *J. Cell Sci.*, **117**, 6535–6546.

Jahn, R. and Scheller, R. H. (2006) SNAREs–engines for membrane fusion. *Nat. Rev. Mol. Cell Biol.*, **7**, 631 – 643.

Karbowski, D., Arnoult, H., Chen, D.C., Chan, C.L., Smith, R.J., Youle, (2004) Quantitation of mitochondrial dynamics by photolabeling of individual organelles shows that mitochondrial fusion is blocked during the Bax activation phase of apoptosis. *J. Cell Biol.*, **164**, 493–499

Klockow, B., Tichelaar, W., Madden, D.R., Niemann, H.H., Akiba, T., Hirose, K., Manstein, D.J. The dynamin A ring complex: molecular organization and nucleotide-dependent conformational changes. (2002) *EMBO J.*, **21**, 240–250.

Koch, G.L.E. and Booth, C. (1988) Dissociation and re-assembly of the endoplasmic reticulum in live cells. *J. Cell Sci.*, **91**, 511–522.

Kondylis, V., Goulding, S. E., Dunne, J. C. & Rabouille, C. (2001) Biogenesis of Golgi stacks in imaginal discs of *Drosophila melanogaster*. *Mol. Biol. Cell*, **12**, 2308-27.

Koshiba, T., Detmer, S., Kaiser, J., Chen, H., McCaffery, J., Chan, D. (2004) Structural basis of mitochondrial tethering by mitofusin complexes acting in trans, *Science*, **305**, 858–862.

Latterich, M., Frolich, K.U. and Schekman, R. (1995) Membrane fusion and the cell cycle; Cdc48p participates in the fusion of ER membranes. *Cell*, **82**, 885–893.

Lee, S. & Cooley, L. (2007) Jagunal is required for reorganizing the endoplasmic reticulum during *Drosophila* oogenesis. J Cell Biol 176, 941-52.

Lee, C., Ferguson, M. and Chen, L.B. (1989) Construction of the endoplasmic reticulum. *J. Cell Biol.*, **109**, 2045–2055.

Lee, Y., D. Paik, *et al.* (2006). Loss of spastic paraplegia gene atlastin induces age-dependent death of dopaminergic neurons in *Drosophila*. *Neurobiol Aging*, **29**(1):84-94.

Lee, M., Paik, S., Lee, M., Kim, Y., Kim, S., Nahm, M., Oh, S., Kim, H., Yim, J., Lee, J., Bae, Y., Lee, S. (2009) *Drosophila* Atlastin regulates the stability of muscle microtubules and is required for synapse development. *Developmental Biology*, **330**, 250–262.

Legros, F., Lombes, A., Frachon, P., Rojo, M. (2002) Mitochondrial fusion in human cells is efficient, requires the inner membrane potential, and is mediated by mitofusins. *Mol. Biol. Cell*, **13**, 4343–4354.

Lindholm, D., Wootz, H. & Korhonen, L. (2006) ER stress and neurodegenerative diseases. *Cell Death Differ*, **13**, 385-92.

Lu, X., Zhang, Y., and Shin, Y. (2008) Supramolecular SNARE assembly precedes hemifusion in SNARE-mediated membrane fusion. *Nat Struct Mol Biol*, **7**, 700–706.

Malsam, J., Kreye, S. and Sçllner, T. H. (2008) Membrane fusion: SNAREs and regulation. *Cell. Mol. Life Sci.*, **65**(18):2814-32.

Meeusen, S., McCaffery, J.M., Nunnari, J. (2004) Mitochondrial fusion intermediates revealed *in vitro*. *Science*, **305**, 1747–1752.

Martens, S. and McMahon, H. T. (2008) Mechanisms of membrane fusion: disparate players and common principles. *Nature Reviews Mol. Cell Biol.*, **9**(7):543-56

McNew, J. A., Weber, T., Engelman, D.M., Sollner, T. H. and Rothman, J. E. (1999) The length of the flexible SNAREpin juxtamembrane region is a critical determinant of SNAREdependent fusion. *Mol. Cell.* **4**, 415 – 421.

McNew, J. A., Weber, T., Parlati, F., Johnston, R. J., Melia, T. J., Sollner, T. H. and Rothman, J. E. (2000) Close is not enough: SNARE-dependent membrane fusion requires an active mechanism that transduces force to membrane anchors. *J. Cell Biol.*, **150**, 105 – 117.

Muhlberg, A.B., Warnock, D.E. and Schmid, S.L. (1997)Domain structure and intramolecular regulation of dynamin GTPase. *EMBO Journal*, **16**, 6676–6683.

Namekawa, M., Muriel, M. P., Janer, A., Latouche, M., Dauphin, A., Debeir, T., Martin, E., Duyckaerts, C., Prigent, A., Depienne, C., Sittler, A., Brice, A., Ruberg, M. (2007) Mutations in the SPG3A gene encoding the GTPase atlastin interfere with vesicle trafficking in the ER/Golgi interface and Golgi morphogenesis. *Mol Cell Neurosci*, **35**(1): 1-13

Namekawa, M., Ribai, P., Nelson, I., Forlani, S., Fellmann, F., Goizet, C., Depienne, C., Stevanin, G., Ruberg, M., Dürr, A., Brice, A., (2006) SPG3A is the most frequent cause of hereditary spastic paraplegia with onset before age 10 years. *Neurology*, **66**, 112–114.

Niemann, H.H., Knetsch, M.L., Scherer, A., Manstein, D.J., Kull, F.J. (2001) Crystal structure of a dynamin GTPase domain in both nucleotide-free and GDP-bound forms. *EMBO J.* **20**, 5813–5821.

Nunnari, J., Marshall, W., Straight, A., Murray, A., Sedat, J.W., Walter, P. (1997) Mitochondrial transmission during mating in S. cerevisiae is determined by mitochondrial fusion and fission and the intramitochondrial segregation of mtDNA. *Mol. Biol. Cell*, **8**, 1233–1242.

Olichon, A. Emorine, L.J., Descoins, E., Pelloquin, L., Brichese, L., Gas, N., Guillou, E., Delettre, C., Valette, A., Hamel, C.P., Ducommun, B., Lenaers, G., Belenguer, P. (2002) The human dynamin-related protein OPA1 is anchored to the mitochondrial inner membrane facing the inter-membrane space. *FEBS Lett.*, **523**, 171–176.

Prinz, W.A., Grzyb, L., Veenhuis, M., Kahana, J.A., Silver, P.A. and Rapoport, T.A. (2000) Mutants affecting the structure of the cortical endoplasmic reticulum in *Saccharomyces cerevisiae*. *J. Cell Biol.*, **150**, 461–474.

Praefcke, G. J. and H. T. McMahon (2004). The dynamin superfamily: universal membrane tubulation and fission molecules? *Nat Rev Mol Cell Biol*, **5**(2): 133-47.

Prakash, B., Praefcke, G.J., Renault, L., Wittinghofer, A., Herrmann, C. (2000) Structure of human guanylate-binding protein 1 representing a unique class of GTP-binding proteins. *Nature*, **403**, 567–571.

Reiter, L.T., Potocki, L., Chien, S., Gribskov, M., Bier, E. (2001) A systematic analysis of human disease-associated gene sequences in *Drosophila melanogaster*. *Genome Res*, **11**, 1114– 1125.

Rismanchi, N., Soderblom, C., Soderblom, C., Stadler, J., Zhu, P.P., Blackstone, C. (2008). Atlastin GTPases are required for Golgi apparatus and ER morphogenesis. *Hum Mol Genet*, **17**(11): 1591-604.

Rojo, M., Legros, F., Chateau, D. & Lombes, A. (2002) Membrane topology and mitochondrial targeting of mitofusins, ubiquitous mammalian homologs of the transmembrane GTPase Fzo. *J. Cell Sci.* **115**, 1663–1674.

Roy, L., Bergeron, J.J., Lavoie, C., Hendriks, R., Gushue, J., Fazel, A., Pelletier, A., Morré, D.J., Subramaniam, V.N., Hong, W., Paiement, J. (2000) Role of p97 and Syntaxin 5 in the assembly of transitional endoplasmic reticulum. *Mol. Cell. Biol.*, **11**, 2529–2542.

Shorter, J., Beard, M. B., Seemann, J., Dirac-Svejstrup, A. B. and Warren, G. (2002). Sequential tethering of Golgins and catalysis of SNAREpin assembly by the vesicle-tethering protein p115. *J. Cell Biol.*, **157**, 45 – 62.

Sollner, T., Bennett, M. K.,Whiteheart, S.W., Scheller, R. H. and Rothman, J. E. (1993a). A protein assembly-disassembly pathway *in vitro* that may correspond to sequential steps of synaptic vesicle docking, activation, and fusion. *Cell*, **75**, 409 – 418.

Sollner, T., Whiteheart, S. W., Brunner, M., Erdjument-Bromage, H., Geromanos, S., Tempst, P. and Rothman, J. E. (1993b). SNAP receptors implicated in vesicle targeting and fusion. *Nature*, **362**, 318 – 324.

Stanley, H., Botas, J. & Malhotra, V. (1997) The mechanism of Golgi segregation during mitosis is cell type-specific. *Proc Natl Acad Sci U S A*, **94**, 14467-70.

Südhof, T., Rothman, J.E. (2009) Membrane Fusion: Grappling with SNARE and SM Proteins. *Science*, **323**, 474.

Sztul, E. and Lupashin, V. (2006). Role of tethering factors in secretory membrane traffic. *Am. J. Physiol. Cell Physiol.*, **290**, C11 – 26.

Terasaki, M. (2000) Dynamics of the endoplasmic reticulum and Golgi apparatus during early sea urchin development. *J. Cell Biol.*, **114**, 929–940.

Terasaki, M., Chen, L.B. and Fujiwara, K. (1986) Microtubules and the endoplasmic reticulum are highly interdependent structures. *J. Cell Biol.*, **103**, 1557–1568.

Terasaki, M. and Jaffe, L.A. (1991) Organization of the sea urchin egg endoplasmic reticulum and its reorganization at fertilization. *J. Cell Biol.*, **114**, 929–940.

Terasaki, M., Slater, N.T., Fein, A., Schmidek, A. and Reese, T.S. (1994) Continuous network of endoplasmic reticulum in cerebellar Purkinje neurons. *Proc. Natl Acad. Sci. USA*, **91**, 7510–7514.

Thor, S. (1995) The genetics of brain development: conserved programs in flies and mice. *Neuron* **15:** 975–977

Vedrenne, C. & Hauri, H. P. (2006) Morphogenesis of the endoplasmic reticulum: beyond active membrane expansion. *Traffic*, **7**, 639-46.

Venken KJ, Bellen HJ (2005) Emerging technologies for gene manipulation in *Drosophila melanogaster*. *Nat Rev Genet* **6:** 167–178.

Voeltz, G. K., Prinz, W. A., Shibata, Y., Rist, J. M. & Rapoport, T. A. (2006) A class of membrane proteins shaping the tubular endoplasmic reticulum. *Cell*, **124**, 573-86.

Voeltz, G. K., Rolls, M. M. & Rapoport, T. A. (2002) Structural organization of the endoplasmic reticulum. *EMBO Rep*, **3**, 944-50.

Wakefield, S. and Tear, G. (2006) The *Drosophila* reticulon, Rtnl-1, has multiple differentially expressed isoforms that are associated with a sub-compartment of the endoplasmic reticulum. *Cell Mol Life Sci*, **63**, 2027-38.

Ward, T. H., Polishchuk, R. S., Caplan, S., Hirschberg, K. and Lippincott-Schwartz, J. (2001) Maintenance of Golgi structure and function depends on the integrity of ER export. *J Cell Biol*, **155**, 557-70.

Waterman-Storer, C.M. and Salmon, E.D. (1998) Endoplasmic reticulum membrane tubules are distributed by microtubules in living cells using three distinct mechanisms. *Curr. Biol.*, **8**, 798–806.

Weber, T., Parlati, F., McNew, J. A., Johnston, R. J., Westermann, B., Sçllner, T. H. and Rothman, J. E. (2000) SNAREpins are functionally resistant to disruption by NSF and alphaSNAP. *J. Cell Biol.*, **149**, 1063 – 1072.

Weber, T., Zemelman, B. V., McNew, J. A., Westermann, B., Gmachl, M., Parlati, F., Sçllner, T. H. and Rothman, J. E. (1998). SNAREpins: minimal machinery for membrane fusion. *Cell*, **92**, 759 – 772.

Wilhelm, J. E., Buszczak, M. and Sayles, S. (2005) Efficient protein trafficking requires trailer hitch, a component of a ribonucleoprotein complex localized to the ER in *Drosophila*. *Dev. Cell*, **9**, 675-85.

Xu,Y., Zhang, F., Su, Z., McNew, J.A. and Shin,Y. K. (2005) Hemifusion in SNARE-mediated membrane fusion. *Nat. Struct. Mol. Biol*., **12**, 417 – 422.

Yoon, Y., Pitts, K. R. and McNiven, M. A. (2001) Mammalian dynamin-like protein DLP1 tubulates membranes. *Mol. Biol. Cell*, **12**, 2894–2905.

Zhao, X., D. Alvarado, D., Rainier, S., Lemons, R., Hedera, P., Weber, C.H., Tukel, T., Apak, M., Heiman-Patterson, T., Ming, L., Bui, M., Fink, J.K. (2001). Mutations in a newly identified GTPase gene cause autosomal dominant hereditary spastic paraplegia. *Nat. Genet.*, **29**(3): 326-3.

Zhu, P.P., Patterson, A., Lavoie, B., Stadler, J., Shoeb, M., Patel, R., Blackstone, C., (2003) Cellular localization, oligomerization, and membrane association of the hereditary spastic paraplegia 3A (SPG3A) protein atlastin. *J. Biol. Chem.*, **278**, 49063–49071.

Zhu, P. P., C. Soderblom, Soderblom, C., Tao-Cheng, J.H., Stadler, J., Blackstone, C. (2006) SPG3A protein atlastin-1 is enriched in growth cones and

promotes axon elongation during neuronal development. *Hum. Mol. Genet*., **15**(8): 1343-53.

Acknowledgements:

Thanks to Andrea Daga’s laboratory. Thanks to James A. McNew for liposome fusion assay. Thanks to Roman S. Polishchuk and Massimo Micaroni for EM experiments.